

SARS-CoV spike protein-expressing recombinant vaccinia virus efficiently induces neutralizing antibodies in rabbits pre-immunized with vaccinia virus

Masahiro Kitabatake^{a,b}, Shingo Inoue^c, Fumihiko Yasui^a, Shoji Yokochi^{a,d}, Masaaki Arai^{a,e}, Kouichi Morita^c, Hisatoshi Shida^f, Minoru Kidokoro^g, Fukashi Murai^d, Mai Quynh Le^h, Kyosuke Mizunoⁱ, Kouji Matsushima^b, Michinori Kohara^{a,*}

^a Department of Microbiology and Cell Biology, The Tokyo Metropolitan Institute of Medical Science, 3-18-22, Honkomagome, Bunkyo-ku, Tokyo 113-8613, Japan

^b Department of Molecular Preventive Medicine, School of Medicine, The University of Tokyo, 7-3-1, Hongo, Bunkyo-ku, Tokyo 113-0033, Japan

^c Department of Virology, Institute of Tropical Medicine, Nagasaki University, 1-12-4, Sakamoto, Nagasaki 852-8523, Japan

^d Post Genome Institute Co., Ltd., 3-38-1, Hongo, Bunkyo-ku, Tokyo 113-0033, Japan

^e Pharmaceuticals Research Unit, Research & Development Division, Mitsubishi Pharma Corporation, 1000, Kamoshida-cho, Aoba-ku, Yokohama 227-0033, Japan

^f Division of Molecular Virology, Institute for Genetic Medicine, Hokkaido University, N15 W7, Kita-ku, Sapporo 060-0815, Japan

^g Third Department of Virology, National Institute of Infectious Diseases, 4-7-1, Gakuen, Musashimurayama 208-0011, Japan

^h Department of Virology, National Institute of Hygiene and Epidemiology, Hanoi, Vietnam

ⁱ The Chemo-Sero-Therapeutic Research Institute, 1-6-1, Okubo, Kumamoto 860-8568, Japan

Received 15 May 2006; received in revised form 20 July 2006; accepted 19 August 2006

Available online 11 September 2006

Abstract

A vaccine for severe acute respiratory syndrome (SARS) is being intensively pursued against its re-emergence. We generated a SARS coronavirus (SARS-CoV) spike protein-expressing recombinant vaccinia virus (RVV-S) using highly attenuated strain LC16m8. Intradermal administration of RVV-S into rabbits induced neutralizing (NT) antibodies against SARS-CoV 1 week after administration and the NT titer reached 1:1000 after boost immunization with RVV-S. Significantly, NT antibodies against SARS-CoV were induced by administration of RVV-S to rabbits that had been pre-immunized with LC16m8. RVV-S can induce NT antibodies against SARS-CoV despite the presence of NT antibodies against VV. These results suggest that RVV-S may be a powerful SARS vaccine, including in patients previously immunized with the smallpox vaccine.

© 2006 Elsevier Ltd. All rights reserved.

Keywords: SARS coronavirus; Recombinant vaccinia virus; LC16m8

1. Introduction

In November 2002, an influenza-like acute pneumonia designated as severe acute respiratory syndrome (SARS) by the World Health Organization, first emerged in China and spread to 29 countries within a few months. By July 2003, 8098 probable cases with 774 deaths were

reported (www.cdc.gov/mmwr/mguide_sars.html). The etiologic agent of SARS was identified as a novel type of coronavirus (CoV) that was genetically distinct from previously characterized members of the Coronaviridae family [1–3]. Like other coronaviruses, SARS-CoV is a positive stranded RNA virus with an approximately 30 kb genome encoding non-structural proteins as well as structural proteins, including spike, envelope, membrane and nucleocapsid. Spike protein is a type I transmembrane glycoprotein that mediates binding to the host cell receptor using an amino-terminal S1

* Corresponding author. Tel.: +81 3 4463 7589; fax: +81 3 3828 8945.
E-mail address: mkohara@rinshoken.or.jp (M. Kohara).

domain and membrane fusion using a carboxyl-terminal S2 domain [4]. Angiotensin-converting enzyme 2 (ACE2) binds to the S1 domain of SARS-CoV spike protein and functions as a receptor for SARS-CoV [5]. CoV spike protein is a major target of protective immunity [6], and neutralizing (NT) antibodies and cytotoxic T lymphocytes against SARS-CoV spike protein have been detected in SARS patients [7,8]. These findings indicate that SARS-CoV spike protein is an appropriate target for vaccines and therapy.

The SARS epidemic broke in May 2003. However, several cases of SARS were reported in China in 2004. Although the civet cat and bats are suspected to be the natural hosts of SARS-CoV, the reservoir of SARS-CoV has yet to be identified [9–11]. In addition, the precise mechanism underlying the development of SARS is not clear and the therapeutic guidelines for SARS have not been established. It has been reported that prophylactic and therapeutic treatment with pegylated IFN- α reduces viral replication and excretion in SARS-CoV infected macaques [12]. Although pegylated IFN- α may eventually become a good therapeutic agent for SARS after infection, it cannot provide long-term protection when used as a prophylactic agent. Therefore, the development of a SARS vaccine is imperative. Several groups have reported a number of SARS vaccine candidates, including inactivated SARS-CoV vaccines [13,14], DNA vaccines [15,16] and recombinant viral vaccines [17–19] expressing one or more SARS-CoV structural proteins. Recombinant live viral vaccines can generally induce strong and long-term immunity, similar to an attenuated live vaccine, and can be abundantly manufactured in a short period of time. More importantly, a safe vaccine can be developed using an attenuated strain that has already been proven safe.

Vaccinia virus (VV) is a double stranded DNA virus with an approximately 180 kb genome, and attenuated strains have been used as the smallpox vaccine. A long DNA fragment is able to be inserted into the VV genome by homologous recombination without damaging viral integrity, as the VV genome is large and contains genes non-essential for viral replication. In fact, recombinant VV can express various proteins encoded by the transduced gene, including the glycosylated proteins of pathogens, some of which have been evaluated as candidates for prophylactic and therapeutic vaccines [20]. Lister is the attenuated VV strain that was used in the worldwide smallpox eradication program. However, additional attenuated strains were generated from Lister due to its side effects, which included erythema, fever and encephalitis. LC16m8 was isolated from Lister via the intermediate strains, LC16 and LC16mO, by multiple plaque purification in primary rabbit kidney cells. LC16m8 is characterized by temperature sensitivity and the formation of small pocks [21]. No serious side effects were observed among the over 100,000 people who were immunized with LC16m8, while the immunogenicity of LC16m8 is similar to that of Lister [22]. Therefore, LC16m8 was authorized as the vaccine against smallpox by the Japanese Ministry of Health and Welfare in 1975.

Recombinant VV expresses proteins encoded by transduced genes under the control of its own promoters. Highly efficient hybrid promoters have been developed and are composed of poxvirus A-type inclusion body (ATI) late promoter and tandem repeats of mutated 7.5 kDa protein (p7.5) early promoter [23]. The protein expressed under the control of the ATI/p7.5 hybrid promoter strongly induces both humoral and cellular immunity [24]. In the present study, we generated a recombinant VV expressing SARS-CoV spike protein (RVV-S) under the control of the ATI/p7.5 hybrid promoter, using LC16m8, and examined whether RVV-S could be used as a SARS vaccine.

2. Materials and methods

2.1. Viruses and cells

SARS-CoV (Vietnam/NB-04/2003 strain), which was isolated from nasal and throat swabs from 1 patient in Hanoi, has been previously described [25]. LC16m8 and LC16mO were kindly provided by the Chemo-Sero-Therapeutic Research Institute (Kumamoto, Japan). The RK13 cell line (ATCC: CCL-37) and VERO E6 cell line (ATCC: CRL-1586) were cultured in MEM (Nissui Pharmaceutical Co. Ltd., Tokyo, Japan) containing 5% fetal bovine serum.

2.2. Generation of recombinant vaccinia virus

The pSFJ1-10 vector contains the ATI/p7.5 hybrid promoter within the hemagglutinin (HA) gene region of VV [23]. Full length cDNA encoding the SARS-CoV spike protein gene was cloned from SARS-CoV viral RNA by RT-PCR, and then inserted downstream of the ATI/p7.5 hybrid promoter of pSFJ1-10; final designation: pSFJ1-10-SARS-S. pSFJ1-10-SARS-S was then transfected into RK13 cells that had been infected with LC16m8 at a multiplicity of infection (moi) of 10 plaque forming units (PFU)/cell. At 24 h after transfection, the virus was harvested. HA negative plaques were cloned as described previously [26]. Briefly, the harvested virus was re-infected into RK13 cells. At 96 h after infection, cells were washed with PBS (+) twice, and then incubated with chicken erythrocytes for 30 min at 30°C. Following washing again with PBS (+), white plaques were isolated. Isolated viruses were cloned by three serial rounds of plaque purification using erythrocyte agglutination and then propagated in RK13 cells. Insertion of the SARS-CoV spike protein gene into LC16m8 genome was confirmed by direct PCR and expression was detected by Western blotting. The viral titer of RVV-S was determined using the standard plaque assay.

2.3. Western blotting

RK13 cells were infected with RVV-S or LC16m8 at moi 10. After 24 h infection, cells were lysed with RIPA

Table 1
Immunization schedule of RVV-S and LC16m8

Rabbit #	0 week		6 weeks		12 weeks		18 weeks	
	Virus	Dose (PFU)	Virus	Dose (PFU)	Virus	Dose (PFU)	Virus	Dose (PFU)
R1–R3	RVV-S	10 ⁸	RVV-S	10 ⁸				
R4–R6	LC16m8	10 ⁸	LC16m8	10 ⁸	RVV-S	10 ⁸	RVV-S	10 ⁸
R7–R9	RVV-S	10 ⁶	RVV-S	10 ⁶				
R10–R12	RVV-S	10 ⁷	RVV-S	10 ⁷				
R13–R15	LC16m8	10 ⁷	RVV-S	10 ⁷	RVV-S	10 ⁷		

buffer (10 mM Tris, pH 7.4, 150 mM NaCl, 1% SDS and 0.5% Nonidet-P40), and 30 µg of total protein was subjected to 7.5% SDS-PAGE and was transferred to a polyvinylidene difluoride membrane (Immobilon-P, Millipore, Bedford, MA). The membrane was blocked in 5% skim milk in TBS containing 0.1% Tween-20 (TBS-T) and then washed with TBS-T. Polyclonal antibodies against spike protein were used as the primary antibody. These were prepared from rabbit sera immunized with a KLH-conjugated spike protein peptide (amino acid residues 559–570 or 1236–1248) and the IgG fraction purified using the Ampure PA kit (Amersham Bioscience, Piscataway, NJ). Antigen-antibody interaction was detected by horseradish peroxidase (HRP)-conjugated donkey anti-rabbit polyclonal antibodies (Amersham Bioscience) and visualized using the ECL system (Amersham Bioscience).

2.4. Immunofluorescence analysis

RK13 cells seeded on slide-glass were infected with RVV-S or LC16m8 at moi 5. At 12 h after incubation at 30 °C, cells were fixed in cold acetone/methanol and then blocked in 1% BSA in PBS (–) for 1 h at room temperature. Following removal of the blocking buffer, cells were incubated with polyclonal antibodies against spike protein, which recognize the C-terminal peptide of spike protein (amino acid residues 1236–1248), for 1 h at room temperature. Following three washes with PBS containing 0.05% Tween-20 (PBS-T), cells were incubated with Alexa 488-conjugated anti-rabbit IgG (Invitrogen, Carlsbad, CA) for 1 h at room temperature. After washing again with PBS-T, the slide-glasses were mounted in Permafluor (Beckman Coulter, Fullerton, CA) containing 1 µg/ml 6-diamidino-2-phenylindole (DAPI) and analyzed using a confocal microscope (LSM510, Carl Zeiss, Oberkochen, Germany).

2.5. Immunization of rabbits

Groups of three New Zealand White rabbits, which were purchased from SLC (Hamamatsu, Japan), were intradermally immunized with one of several doses (10⁶, 10⁷ or 10⁸ PFU) of RVV-S, or with 10⁸ PFU of LC16m8, at 0 and 6 weeks. The LC16m8 immunized group was further immunized with 10⁸ PFU of RVV-S at 12 and 18 weeks. Another group of three rabbits was immunized with 10⁷ PFU of LC16m8 at 0 week, and then immunized with 10⁷ PFU of

RVV-S at 6 and 12 weeks. A summary of the immunization schedule is shown in Table 1. Sera were collected every week, and used for enzyme linked immunosorbent assay (ELISA) and the *in vitro* neutralization (NT) assay below. All animal experiments were approved by The Tokyo Metropolitan Institute of Medical Science Animal Experiment Committee and were performed in accordance with the animal experimentation guidelines of The Tokyo Metropolitan Institute of Medical Science.

2.6. ELISA

Full length recombinant SARS-CoV spike protein containing a six-histidine tag (His) was expressed in RK13 cells by RVV-S-His, which was generated from LC16mO, and purified using Nickel sepharose (Amersham Bioscience). Peptides from the N-terminal (mixture of three peptides, amino acid residues 12–53, 90–115 and 171–203), middle position (mixture of two peptides, amino acid residues 408–470 and 540–573) and C-terminal (mixture of three peptides, amino acid residues 1051–1076, 1121–1154 and 1162–1190) of the spike protein, which respond to sera from SARS-infected individuals, were purchased from ProSpec-Tany TechnoGene Ltd. (Rehovot, Israel). These three peptide mixtures or full length spike protein were coated onto the 96 well plates at 4 °C. The plates were blocked with 1% BSA in PBS (–) containing 0.5% Tween-20 and 2.5 mM EDTA, and then incubated with serial dilutions of sera from the rabbits immunized with RVV-S or LC16m8. After extensive washing, the plates were incubated with HRP-conjugated donkey anti-rabbit polyclonal antibodies (Amersham Bioscience). Antigen–antibody interactions were detected using 3,3',5,5'-tetramethylbenzidine solution as the substrate (Becton Dickinson, San Jose, CA), and the binding activity was measured by the absorbance at 450 nm.

2.7. *In vitro* NT assay for SARS-CoV

Serial dilutions of heat-inactivated sera were mixed with equal volumes of 100 TCID₅₀ of SARS-CoV and incubated at 37 °C for 1 h. VERO E6 cells were then infected with the virus/sera mixtures in 96 well plates. At 120 h after infection, the NT titer was determined as the maximum dilution of sera that inhibited the SARS-CoV induced cytopathic effect by more than 50%. All experiments with SARS-CoV were performed in a biosafety containment level III facility.

2.8. In vitro NT assay for VV

Serial dilutions of heat-inactivated sera were mixed with equal volumes of 100 PFU of LC16mO, and incubated at 37 °C for 1 h, followed by incubation at 4 °C for 16 h. RK13 cells were then infected with the virus/sera mixtures in 6 well plates. At 48 h after infection, the NT titer was determined as the maximum dilution of sera that inhibited plaque formation by more than 50%.

2.9. Statistical analysis

All data were expressed as mean \pm S.E.M. Data for RVV-S dose dependent effect were statistically analyzed by one-way ANOVA followed by Turkey test. Data for LC16m8 pre-immunization effect were statistically analyzed by Student's or by Welch's *t*-test. $p < 0.05$ was considered to be statistically significant.

3. Results

3.1. Generation and characterization of RVV-S

The full length SARS-CoV spike protein gene was inserted by homologous recombination into the HA gene region of LC16m8, which was located downstream of the powerful ATI/p7.5 hybrid promoter (Fig. 1A). Recombination between pSFJ1-10-SARS-S and LC16m8 results in inactivation of the HA gene. We screened for RVV-S using the erythrocyte agglutination assay, and insertion of the transduced gene was then confirmed by PCR. To confirm the expression of SARS-CoV spike protein, Western blotting was performed. Two kinds of rabbit polyclonal antibodies that recognized different epitopes, amino acid residues 559–570 and 1236–1248 of SARS-CoV spike protein, were used as the primary antibody. In RVV-S but not LC16m8 infected cells, both antibodies detected an approximately 180 kDa protein (Fig. 1B and C), which is consistent with the molecular mass of spike protein [18]. SARS-CoV spike protein is reported to be highly glycosylated, and thus the molecular mass on SDS-PAGE is larger than that predicted from the gene sequence [18]. Expression of spike protein following infection with RVV-S was also confirmed by immunofluorescence analysis. RVV-S infected VERO E6 cells were stained with antibody against spike protein, whereas no staining was observed in the cells infected with LC16m8 or the uninfected control cells (Fig. 1D).

3.2. Induction of binding antibodies against spike protein in RVV-S-immunized rabbits

To investigate whether RVV-S induces binding antibodies against spike protein, 10^8 PFU of RVV-S or LC16m8 (as the control) was intradermally injected into rabbits at 0 and 6 weeks. Rabbits immunized with either RVV-S or LC16m8

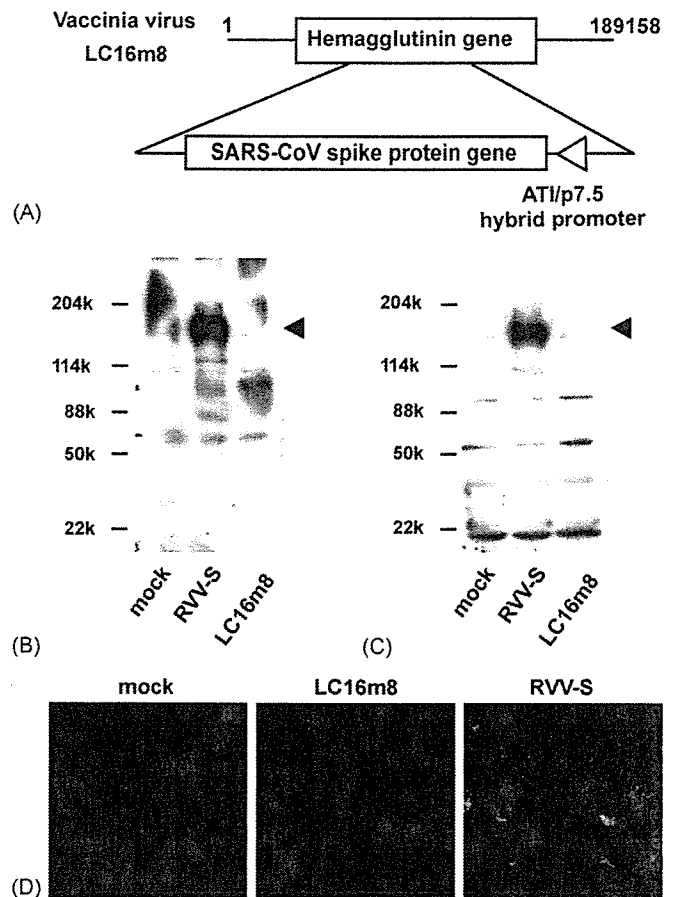


Fig. 1. Characteristics of SARS-CoV spike protein-expressing recombinant vaccinia virus (RVV-S) derived from LC16m8. (A) The full length SARS-CoV spike protein gene was inserted into the HA gene region of the LC16m8 genome. The ATI/p7.5 hybrid promoter regulates expression of spike protein. (B and C) RK13 cells were infected with RVV-S or LC16m8 at moi 10. At 24 h after infection, cells were harvested and analyzed. Two kinds of anti-SARS-CoV spike protein polyclonal antibodies, which recognize different epitopes, namely amino acid residues 559–570 (B) and 1236–1248 (C) of spike protein, were used as the primary antibodies. The molecular masses of marker proteins in kDa are shown on the left and the position of the spike protein is indicated by an arrowhead on the right. (D) Indirect immunofluorescence staining of spike protein. Expression of spike protein was visualized by staining with anti-SARS-CoV spike polyclonal antibodies, followed by Alexa 488-conjugated anti-rabbit IgG (green). Nuclei were stained with DAPI (red).

did not exhibit weight loss or any clinical signs except for regional skin reactions, such as erythema and induration. The skin reaction induced by RVV-S was comparable to that induced by LC16m8 (data not shown). Binding antibodies against full length spike protein were detected by ELISA in the sera from rabbits immunized with RVV-S (Fig. 2A). Next, we investigated the binding activities of immunized sera against different epitopes of the spike protein. RVV-S-immunized sera reacted with all three regions of spike protein. The sera bound to the C-terminal peptides, which contained the heptad repeat 2 (HR2) region, reported to be the NT epitope of SARS-CoV (Fig. 2B) [27] and to the middle peptides,

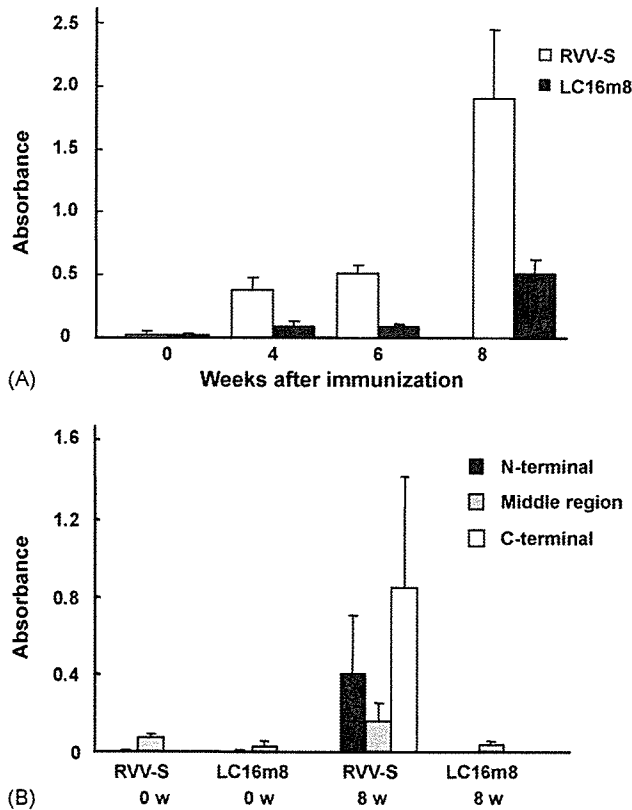


Fig. 2. Induction of binding antibodies against SARS-CoV spike protein. New Zealand White rabbits ($n=3$) were immunized with 10^8 PFU of RVV-S (R1-3; open symbols) or LC16m8 (R4-6; closed symbols) at 0 and 6 weeks. The binding activity of 10^3 - or 10^4 -fold dilutions of immunized sera was assessed using His-tagged full length spike protein (A), or one of three kinds of spike protein partial peptides (B), as the capture antigen.

in which a receptor binding domain, another NT epitope of SARS-CoV, was included [28].

3.3. Induction of NT antibodies against SARS-CoV in RVV-S-immunized rabbits

Next, to determine whether the antibodies induced by immunization with RVV-S have NT activity against SARS-CoV, we performed an *in vitro* NT assay against SARS-CoV using immunized sera. Interestingly, the sera obtained from all three rabbits in this group showed NT activity against SARS-CoV, even at 1 week after immunization with 10^8 PFU of RVV-S (Fig. 3A). The NT titer reached 1:100 at 3 weeks, and increased 10-fold further by boost immunization. In contrast, sera obtained from rabbits immunized with LC16m8 did not show any NT activity against SARS-CoV (Fig. 3A). Next, to determine the minimum dose that can induce NT antibodies against SARS-CoV by single immunization, rabbits were immunized with lower doses of RVV-S. All three rabbits that underwent single immunization with 10^7 PFU of RVV-S generated NT antibodies against SARS-CoV (Fig. 3A). The NT titer further increased by boost immunization with 10^7 PFU of RVV-S and reached a comparable level to that induced by 10^8 PFU of RVV-S (Fig. 3B). On the other hand, NT activity

was induced by single immunization with 10^6 PFU of RVV-S at 2 and 4 weeks after immunization in all three rabbits, but then decreased below the detection limit in one rabbit at 6 weeks (Fig. 3A). However, the NT titer increased to approximately 1:300 in the group immunized with 10^6 PFU of RVV-S by boost immunization with the same dose of RVV-S (Fig. 3B).

3.4. RVV-S induces NT antibodies against SARS-CoV in the presence of NT antibodies against VV

Induction of NT antibodies against VV by RVV-S was next examined. The *in vitro* NT assay against VV revealed that LC16m8 and RVV-S equally induced NT antibodies against VV in the rabbits (Fig. 3C). NT activity against VV was induced by 10^8 PFU of RVV-S at 1 week after immunization, similar to SARS-CoV. The NT titer against VV, which reached 1:10,000 at 2 weeks after boost immunization with 10^8 PFU of RVV-S, was similar to that induced by 10^8 PFU of LC16m8. These results suggest that the epitopes of the NT antibodies against VV were preserved in RVV-S. Since VV has been used as a smallpox vaccine in humans, we were concerned that RVV-S might be eliminated by the host's immune response before inducing effective immunity against a protein encoded by the transduced gene. Therefore, to assess whether RVV-S can induce NT antibodies against SARS-CoV in rabbits that had NT antibodies against VV, RVV-S was injected into rabbits which had been pre-immunized with LC16m8. NT antibodies against VV were induced in the rabbits by single immunization with 10^7 PFU of LC16m8 and the NT titer reached 1:64–256 (Fig. 4A). By following immunization with an equal dose of RVV-S (10^7 PFU), NT antibodies against SARS-CoV were induced in all three rabbits, although induction of NT antibodies was delayed in one rabbit (R14). Although the induction of NT antibodies against SARS-CoV was partially suppressed in the LC16m8 pre-immunized rabbits, the NT titer further increased in all three rabbits by boost immunization with RVV-S (Fig. 4C). These results suggest that RVV-S can induce NT antibodies in individuals who have been previously immunized with a smallpox vaccine. Next, we examined whether RVV-S induced NT antibodies against SARS-CoV in rabbits with a high titer of NT antibodies against VV. The NT titer against VV in rabbits that had been immunized twice with 10^8 PFU of LC16m8 was sustained at approximately 1:4000 (Fig. 4B). Although these rabbits had an extremely high titer of NT antibodies against VV, NT antibodies against SARS-CoV were induced in all three rabbits upon a booster injection with 10^8 PFU of RVV-S (Fig. 4B). Surprisingly, the NT titer of these rabbits increased to levels comparable to those of the non-pre-immunized rabbits (Fig. 4C). These results indicate that an immune response against a protein encoded by a transduced gene can be induced by immunization with 10^8 PFU of RVV in spite of the pre-existence of NT antibodies against VV.

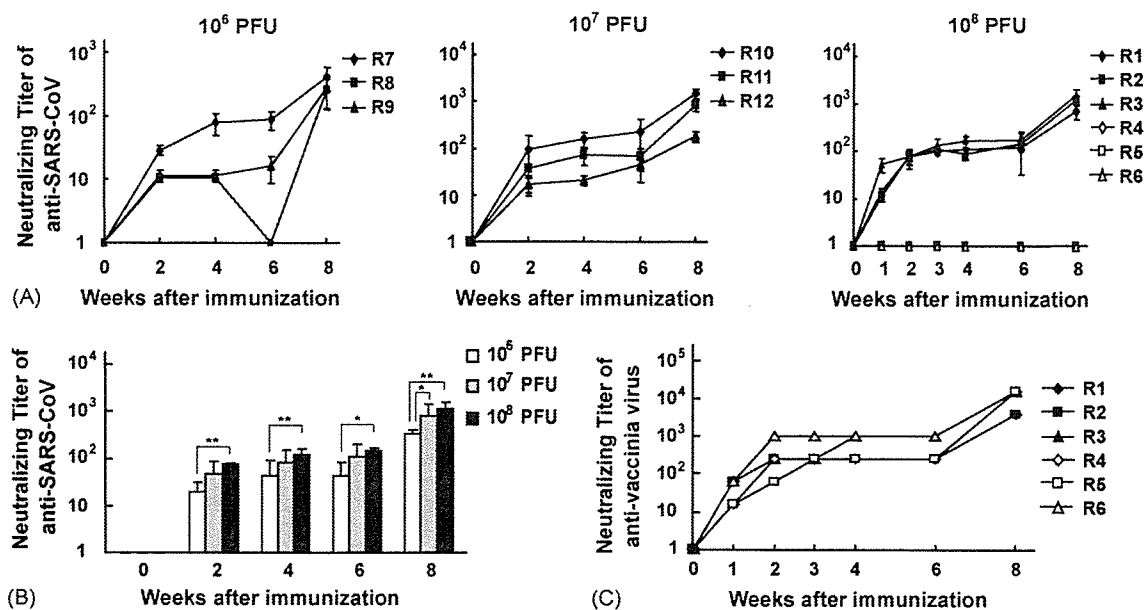


Fig. 3. Induction of NT antibodies against SARS-CoV and vaccinia virus. (A) The NT activity against SARS-CoV of RVV-S- (10^6 PFU, R7–9; 10^7 PFU, R10–12; 10^8 PFU, R1–3; closed symbols) or LC16m8- (R4–6; open symbols) immunized rabbit sera was defined as the maximum dilution of sera that inhibited the cytopathic effect of SARS-CoV by more than 50%. (B) The dose dependency of immunization with RVV-S shown in (A). * $p < 0.05$, ** $p < 0.01$. (C) The NT activity against vaccinia virus of RVV-S- (R1–3, closed symbols) or LC16m8- (R4–6, open symbols) immunized sera was defined as the maximum dilution of sera that inhibited plaque formation by LC16mO by more than 50%.

4. Discussion

In the present study, we generated a SARS-CoV spike protein-expressing recombinant vaccinia virus using a highly attenuated strain, LC16m8, and demonstrated that NT antibodies against SARS-CoV can be strongly induced by immunization with RVV-S, not only in naïve rabbits but also in LC16m8 pre-immunized rabbits.

In a previous study, passive transfer of sera obtained from mice inoculated with SARS-CoV prevented the replication of SARS-CoV in the upper and lower respiratory tract [29]. In addition, intraperitoneal injection of sera from mice immunized with MVA expressing spike protein (MVA/S) reduced the viral titers in lung and nasal turbinate in a dose-dependent manner [18]. These findings indicate that NT antibodies against spike protein are sufficient to protect against SARS-CoV infection. Single immunization with 10^7 or 10^8 PFU of RVV-S and two immunizations with 10^6 PFU of RVV-S were able to induce a high level of NT antibodies against SARS-CoV at 2 weeks after immunization. Therefore, RVV-S also may protect against SARS-CoV *in vivo* and would be a highly effective vaccine against SARS in naïve individuals.

Contrary to the above studies [18,29], Czub et al. [30] reported that immunization with MVA/S did not prevent SARS-CoV infection in ferrets but rather produced inflammatory responses and focal necrosis in the liver after SARS-CoV challenge. This may have been due to only low NT activity against SARS-CoV being induced by the MVA/S immunization. Moreover, the precise mechanism of this liver inflammation has not been clarified. Feline infectious

peritonitis virus (FIPV), another member of the coronaviruses, exhibited enhanced FIPV infection into monocytes/macrophages through viral-specific antibody binding to the Fc receptors of these cells, and caused enhanced inflammation [31]. However, there is no evidence that NT antibodies against SARS-CoV cause antibody-dependent enhancement, and correlation between inflammation and antibody-dependent enhancement by MVA/S vaccination has not yet been established. The side effects of vaccines are also influenced by the dosage and route of immunization. In Czub's report, MVA/S was intraperitoneally injected into the ferrets, although most vaccinations with RVV are conducted through other routes, such as intradermal, intramuscular or subcutaneous injection. Therefore, selection of a different immunization route may prevent such side effects. Nonetheless, further analysis of the side effects of various SARS vaccines, including RVV-S, is required in *in vivo* SARS-CoV challenge models in a variety of animals.

Using RVV-S as a candidate SARS vaccine means that possible complications due to previous vaccination with the VV for smallpox may be avoided. Hammarlund et al. [32] reported that a particular antiviral antibody against poxvirus is maintained for a very long time (possibly for life) by immunization with the smallpox vaccine. Therefore, there was concern that a RVV vaccine would be eliminated by the host antiviral immune response before induction of effective humoral and/or cellular immunity against the protein encoded by the transduced gene. However, immunization with 10^7 PFU of RVV-S induced NT antibodies against SARS-CoV in rabbits that had been immunized with 10^7 PFU

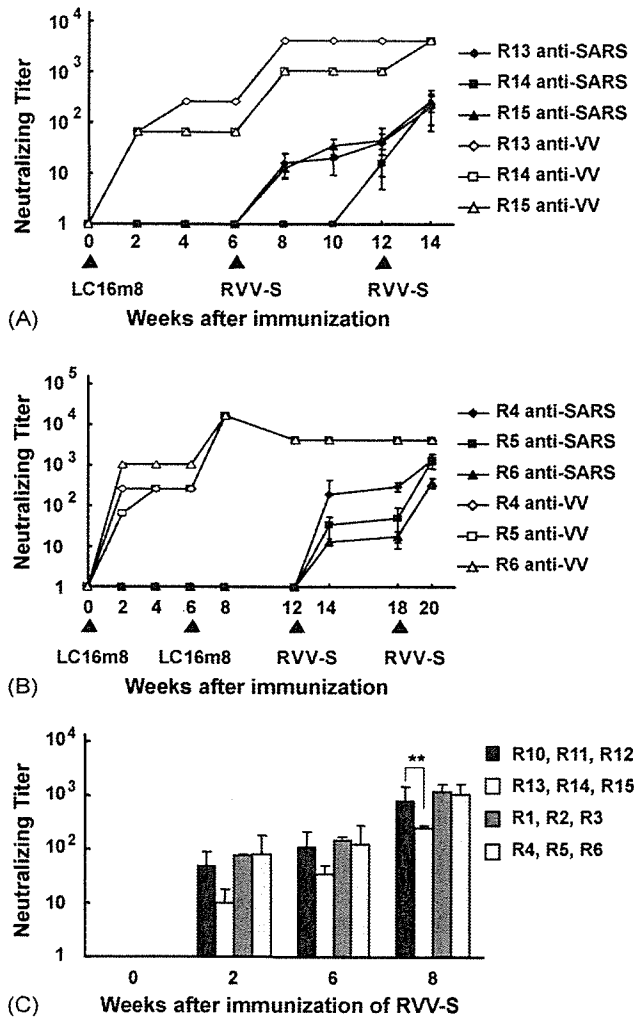


Fig. 4. Induction of NT antibodies against SARS-CoV in rabbits pre-immunized with LC16m8. (A) Three rabbits (R13–15) were immunized with 10^7 PFU of LC16m8 on day 0, and then immunized with 10^7 PFU of RVV-S at 6 and 12 weeks. (B) Three rabbits (R4–6) were immunized with 10^8 PFU of LC16m8 at 0 and 6 weeks, and then immunized with 10^8 PFU of RVV-S at 12 and 18 weeks. Immunized rabbit sera were analyzed by *in vitro* NT assay against SARS-CoV (closed symbols) or vaccinia virus (open symbols). Each type of symbol indicates one and the same individual, and the schedule of immunization with RVV-S or LC16m8 is indicated by arrowheads. (C) Comparison of NT antibodies against SARS-CoV induced by RVV-S in VV-immunized or naïve rabbits. RVV-S (10^7 or 10^8 PFU) was injected into rabbits at 0 and 6 weeks in the presence (10^7 PFU, R13–15; 10^8 PFU, R4–6) or absence (10^7 PFU, R10–12; 10^8 PFU, R1–3) of pre-immunization with an equal titer of LC16m8. Immunized rabbit sera were analyzed by *in vitro* NT assay against SARS-CoV. ** $p < 0.01$.

of LC16m8. Since the NT titer against VV induced by 10^7 PFU of LC16m8 was comparable to that in people vaccinated with the smallpox vaccine [32], RVV-S may induce NT antibodies against SARS-CoV in such people. On the other hand, 10^8 PFU of RVV-S also induced NT antibodies against SARS-CoV in rabbits that had an extremely high titer of NT antibodies against VV due to two pre-immunizations with 10^8 PFU of LC16m8. Furthermore, there was no difference in the NT titer against SARS-CoV induced by RVV-S

between naïve rabbits and LC16m8 pre-immunized rabbits. The immune response against a protein encoded by a transduced gene may be influenced by the amount of antigen expression, the antigenicity of the protein encoded by a transduced gene, the route of immunization and viral proliferation in the host, and thus further analysis is required to resolve the precise mechanism involved. Furthermore, the vaccine effect of RVV-S still needs to be confirmed in humans pre-immunized with the smallpox vaccine.

In the present study, immunization with RVV-S manifested a vaccine effect against SARS-CoV, in spite of the pre-existing NT antibodies against VV. This finding indicates that an RVV vaccine derived from LC16m8 can be used for people previously immunized with the smallpox vaccine. Furthermore, this RVV vaccine could be repeatedly used against various microbes, such as influenza virus, by alteration of the protein encoded by the transduced gene. Therefore, the use of an RVV vaccine generated from LC16m8 is a promising vaccine strategy against various infectious diseases.

Acknowledgments

We thank Y. Sameshima for technical assistance with generation of the recombinant vaccinia virus. We are very grateful to Dr. M. Shuda for helpful discussion. We also thank S. Morikawa of the Department of Virology, National Institute of Infectious Diseases, Tokyo, Japan, for kindly providing the SARS-CoV immunized rabbit sera. This study was supported in part by a Grant for Research on Emerging and Re-emerging Infectious Diseases from the Ministry of Health, Labor and Welfare, Japan, the 21st Century Centers of Excellence [COE] program on Global strategies for Control of Tropical and Emerging Infectious Diseases at Nagasaki University, and the Ministry of Education, Culture, Sports, Science and Technology of Japan.

References

- [1] Drosten C, Gunther S, Preiser W, van der Werf S, Brodt HR, Becker S, et al. Identification of a novel coronavirus in patients with severe acute respiratory syndrome. *N Engl J Med* 2003;348(20):1967–76.
- [2] Ksiazek TG, Erdman D, Goldsmith CS, Zaki SR, Peret T, Emery S, et al. A novel coronavirus associated with severe acute respiratory syndrome. *N Engl J Med* 2003;348(20):1953–66.
- [3] Peiris JS, Lai ST, Poon LL, Guan Y, Yam LY, Lim W, et al. Coronavirus as a possible cause of severe acute respiratory syndrome. *Lancet* 2003;361(9366):1319–25.
- [4] Gallagher TM, Buchmeier MJ. Coronavirus spike proteins in viral entry and pathogenesis. *Virology* 2001;279(2):371–4.
- [5] Li W, Moore MJ, Vasilieva N, Sui J, Wong SK, Berne MA, et al. Angiotensin-converting enzyme 2 is a functional receptor for the SARS coronavirus. *Nature* 2003;426(6965):450–4.
- [6] Spaan W, Cavanagh D, Horzinek MC. Coronaviruses: structure and genome expression. *J Gen Virol* 1988;69(Pt. 12):2939–52.
- [7] Nie Y, Wang G, Shi X, Zhang H, Qiu Y, He Z, et al. Neutralizing antibodies in patients with severe acute respiratory syndrome-associated coronavirus infection. *J Infect Dis* 2004;190(6):1119–26.

- [8] Wang YD, Sin WY, Xu GB, Yang HH, Wong TY, Pang XW, et al. T-cell epitopes in severe acute respiratory syndrome (SARS) coronavirus spike protein elicit a specific T-cell immune response in patients who recover from SARS. *J Virol* 2004;78(11):5612–8.
- [9] Normile D, Enserink M. SARS in China. Tracking the roots of a killer. *Science* 2003;301(5631):297–9.
- [10] Li W, Shi Z, Yu M, Ren W, Smith C, Epstein JH, et al. Bats are natural reservoirs of SARS-like coronaviruses. *Science* 2005;310(5748):676–9.
- [11] Lau SK, Woo PC, Li KS, Huang Y, Tsoi HW, Wong BH, et al. Severe acute respiratory syndrome coronavirus-like virus in Chinese horseshoe bats. *Proc Natl Acad Sci USA* 2005;102(39):14040–5.
- [12] Haagmans BL, Kuiken T, Martina BE, Fouchier RA, Rimmelzwaan GF, van Amerongen G, et al. Pegylated interferon-alpha protects type 1 pneumocytes against SARS coronavirus infection in macaques. *Nat Med* 2004;10(3):290–3.
- [13] Tang L, Zhu Q, Qin E, Yu M, Ding Z, Shi H, et al. Inactivated SARS-CoV vaccine prepared from whole virus induces a high level of neutralizing antibodies in BALB/c mice. *DNA Cell Biol* 2004;23(6):391–4.
- [14] Takasuka N, Fujii H, Takahashi Y, Kasai M, Morikawa S, Itamura S, et al. A subcutaneously injected UV-inactivated SARS coronavirus vaccine elicits systemic humoral immunity in mice. *Int Immunol* 2004;16(10):1423–30.
- [15] Yang ZY, Kong WP, Huang Y, Roberts A, Murphy BR, Subbarao K, et al. A DNA vaccine induces SARS coronavirus neutralization and protective immunity in mice. *Nature* 2004;428(6982):561–4.
- [16] Kim TW, Lee JH, Hung CF, Peng S, Roden R, Wang MC, et al. Generation and characterization of DNA vaccines targeting the nucleocapsid protein of severe acute respiratory syndrome coronavirus. *J Virol* 2004;78(9):4638–45.
- [17] Gao W, Tamin A, Soloff A, D' Aiuto L, Nwanegbo E, Robbins PD, et al. Effects of a SARS-associated coronavirus vaccine in monkeys. *Lancet* 2003;362(9399):1895–6.
- [18] Bisht H, Roberts A, Vogel L, Bukreyev A, Collins PL, Murphy BR, et al. Severe acute respiratory syndrome coronavirus spike protein expressed by attenuated vaccinia virus protectively immunizes mice. *Proc Natl Acad Sci USA* 2004;101(17):6641–6.
- [19] Buchholz UJ, Bukreyev A, Yang L, Lamirande EW, Murphy BR, Subbarao K, et al. Contributions of the structural proteins of severe acute respiratory syndrome coronavirus to protective immunity. *Proc Natl Acad Sci USA* 2004;101(26):9804–9.
- [20] Moss B. Genetically engineered poxviruses for recombinant gene expression, vaccination, and safety. *Proc Natl Acad Sci USA* 1996;93(21):11341–8.
- [21] Sugimoto M, Yasuda A, Miki K, Morita M, Suzuki K, Uchida N, et al. Gene structures of low-neurovirulent vaccinia virus LC16m0, LC16m8, and their Lister original (LO) strains. *Microbiol Immunol* 1985;29(5):421–8.
- [22] Yamaguchi M, Kimura M, Hirayama M. Report of the National Smallpox Vaccination Research Committee: study of side effects, complications and their treatments. *Clin Virol* 1975;3:269–78.
- [23] Jin NY, Funahashi S, Shida H. Constructions of vaccinia virus A-type inclusion body protein, tandemly repeated mutant 7.5 kDa protein, and hemagglutinin gene promoters support high levels of expression. *Arch Virol* 1994;138(3–4):315–30.
- [24] Funahashi S, Itamura S, Iinuma H, Nerome K, Sugimoto M, Shida H. Increased expression in vivo and in vitro of foreign genes directed by A-type inclusion body hybrid promoters in recombinant vaccinia viruses. *J Virol* 1991;65(10):5584–8.
- [25] Hong TC, Mai QL, Cuong DV, Parida M, Minekawa H, Notomi T, et al. Development and evaluation of a novel loop-mediated isothermal amplification method for rapid detection of severe acute respiratory syndrome coronavirus. *J Clin Microbiol* 2004;42(5):1956–61.
- [26] Shida H, Tochikura T, Sato T, Konno T, Hirayoshi K, Seki M, et al. Effect of the recombinant vaccinia viruses that express HTLV-I envelope gene on HTLV-I infection. *Embo J* 1987;6(11):3379–84.
- [27] Keng CT, Zhang A, Shen S, Lip KM, Fielding BC, Tan TH, et al. Amino acids 1055 to 1192 in the S2 region of severe acute respiratory syndrome coronavirus S protein induce neutralizing antibodies: implications for the development of vaccines and antiviral agents. *J Virol* 2005;79(6):3289–96.
- [28] Chen Z, Zhang L, Qin C, Ba L, Yi CE, Zhang F, et al. Recombinant modified vaccinia virus Ankara expressing the spike glycoprotein of severe acute respiratory syndrome coronavirus induces protective neutralizing antibodies primarily targeting the receptor binding region. *J Virol* 2005;79(5):2678–88.
- [29] Subbarao K, McAuliffe J, Vogel L, Fahle G, Fischer S, Tatti K, et al. Prior infection and passive transfer of neutralizing antibody prevent replication of severe acute respiratory syndrome coronavirus in the respiratory tract of mice. *J Virol* 2004;78(7):3572–7.
- [30] Czub M, Weingartl H, Czub S, He R, Cao J. Evaluation of modified vaccinia virus Ankara based recombinant SARS vaccine in ferrets. *Vaccine* 2005;23(17–18):2273–9.
- [31] Olsen CW, Corapi WV, Ngichabe CK, Baines JD, Scott FW. Monoclonal antibodies to the spike protein of feline infectious peritonitis virus mediate antibody-dependent enhancement of infection of feline macrophages. *J Virol* 1992;66(2):956–65.
- [32] Hammarlund E, Lewis MW, Hansen SG, Strelow LI, Nelson JA, Sexton GJ, et al. Duration of antiviral immunity after smallpox vaccination. *Nat Med* 2003;9(9):1131–7.



Original article

CRM1, an RNA transporter, is a major species-specific restriction factor of human T cell leukemia virus type 1 (HTLV-1) in rat cells

Xianfeng Zhang^{a,1}, Yoshiyuki Hakata^{a,2}, Yuetsu Tanaka^b, Hisatoshi Shida^{a,*}^a Institute for Genetic Medicine, Hokkaido University, Kita-15, Nishi-7, Kita-ku, Sapporo 060-0815, Japan^b Department of Immunology, Graduate School and Faculty of Medicine, University of the Ryukyus, Nishihara, Okinawa 903-0215, Japan

Received 5 September 2005; accepted 10 October 2005

Available online 13 January 2006

Abstract

Rat ortholog of human CRM1 has been found to be responsible for the poor activity of viral Rex protein, which is essential for RNA export of human T cell leukemia virus type 1 (HTLV-1). Here, we examined the species-specific barrier of HTLV-1 by establishing rat cell lines, including both adherent and CD4⁺ T cells, which express human CRM1 at physiological levels. We demonstrated that expression of human CRM1 in rat cells is not harmful to cell growth and is sufficient to restore the synthesis of the viral structural proteins, Gag and Env, at levels similar to those in human cells. Gag precursor proteins were efficiently processed to the mature forms in rat cells and released into the culture medium as sedimentable viral particles. An HTLV-1 pseudovirus infection system suggested that the released virus particles are fully infectious. Our newly developed reporter cell system revealed that Env proteins produced in rat cells are fully fusogenic, which is the basis for cell–cell HTLV-1 infection. Moreover, we show that the early steps in infection, from post-entry uncoating to integration into the host chromosomes, occur efficiently in rat cells. These results, in conjunction with reports describing efficient entry of HTLV-1 into rat cells, may indicate that HTLV-1 is unique in that its major species-specific barrier is determined by CRM1 at a viral RNA export step. These observations will enable us to construct a transgenic rat model expressing human CRM1 that is sensitive to HTLV-1 infection.

© 2006 Elsevier SAS. All rights reserved.

Keywords: Human T cell leukemia virus type 1; CRM1; Species barrier

1. Introduction

The human T lymphotropic virus type 1 (HTLV-1) is a type C retrovirus, whose etiological role in adult T cell leukemia (ATL) and tropical spastic paraparesis/HTLV-1 associated myelopathy (TSP/HAM) has been well established [1,2]. In its small genome, the virus encodes not only viral structural and enzymatic proteins, but also several regulatory proteins, using alternative splicing and alternate codon usage. The actions of these regulatory proteins are critical for the virus

life cycle. Tax, identified as a viral onco-protein, activates viral and cellular transcription to promote T-cell growth and ultimately, malignant transformation [3,4]. Rex, which is a nucleocytoplasmic shuttling protein, mediates nuclear export of unspliced or incompletely spliced viral mRNAs, which encode the viral structural and enzymatic proteins, Gag, Pol and Env [5–7]. In the nucleus, Rex interacts with the Rex response element (RxRE), which is located in the 3' long terminal repeat (LTR) of the viral mRNA [8,9]. To form an export complex, Rex binds to human CRM1 (hCRM1), a member of the karyopherin family of nuclear transport receptors, in cooperation with a GTP-bound form of the small G protein Ran (Ran-GTP) and RanBP3 [10–12]. Moreover, multimerization of Rex on the viral RNA is critical for its full biological activity [13], since the Rex multimer may shield the viral RNA from being spliced or down-regulated [14]. Previously, we reported that hCRM1 is dually involved in both the export of the target

* Corresponding author. Tel./fax: +81 11 706 7543.

E-mail address: hshida@igm.hokudai.ac.jp (H. Shida).¹ Current address: Retrovirus Research Unit, RIKEN, Wako, Saitama 351-0198, Japan.² Current address: Infectious Disease Laboratory, The Salk Institute for Biological Studies, La Jolla, CA 92037, USA.

viral mRNA complex and the multimerization of Rex on the cognate RNA [11]. This suggests that hCRM1 is the most critical cofactor guiding Rex function.

Several animal models to investigate the mechanisms underlying the onset of HTLV-1 related diseases have been developed over the past years. Monkeys and rabbits have been used to examine HTLV-1 infection, replication, disease manifestation, immune response, and vaccine development [15–20]. However, rats and mice are more attractive models for HTLV-1 study because of the ease with which they can be genetically manipulated. HTLV-1 transmission to newborn mice has been reported and the HTLV-1 provirus in mouse spleen has been detected [21]. Nevertheless, no viral expression or antibody production was detected in these mice and, furthermore, mouse cells seem to be less susceptible to HTLV-1 envelope fusion [22,23], even though some conflicting results have been reported [24]. In contrast, HTLV-1 infection in rats establishes a persistent infection and elicits specific antibody responses [25,26]. Moreover, HAM/TSP-like diseases develop in HTLV-1-infected WKA/H rats [27,28]. However, until now, efficient replication of HTLV-1 in rat cells has not been reported.

To develop better rat models, it is essential to identify the step at which viral replication is blocked and the host factor(s) responsible. HTLV-1 has been reported to infect several types of rat cells, which indicates that the rat cells possess receptors for viral attachment and penetration [29–31]. Recent identification of a highly conserved molecule, Glut-1, a glucose transporter, as a receptor [32] is consistent with these observations. Previously, we found the inability of the host factor rat CRM1 to support Rex function and thus that viral RNA export from nucleus was a possible block in the viral life cycle. Rat CRM1 induces minimal amount of Rex multimerization on cognate RNA, although it efficiently exports Rex protein to the cytoplasm. This may cause the defect in viral RNA transport [33]. Two residues (amino acids 411 and 414) in the central region of human CRM1 are crucial for multimerization [34]. These results suggest that a transgenic (Tg) rat, which expresses human CRM1, may be a model animal to support replication of HTLV-1. Prior to constructing the Tg rat, we examined the effects of hCRM1, expressed at physiological levels in rat cells, because the above results were obtained by overexpression of human and rat CRM1 and toxic effects from overexpressed CRM1 and a dominant-negative influence of rCRM1 over hCRM1 have been reported [33,35]. Moreover, an understanding of the entire viral life cycle is needed. In the case of the human immunodeficiency virus (HIV), non-human cells have been reported to contain inhibitors such as Trim5 α and Apobec3G, which act at uncoating and reverse-transcription steps, respectively [36,37].

In this study, we constructed rat cells expressing hCRM1 at physiological levels and examined the effects on HTLV-1 replication. We investigated the early steps of the HTLV-1 life-cycle, between entry and transcription, and the late steps, including formation of infectious virus and cell to cell infection. To investigate these steps quantitatively, we used a pseudovirus system [38] and our newly devised cell fusion assay,

because the extremely poor infectivity of free HTLV-1 virions [38,39] makes it impractical to evaluate them by conventional virological methods. Here, we show that expression of hCRM1 in rat cells may be sufficient to enhance production of HTLV-1 proteins and infectious viruses at levels similar to those in human cells.

2. Materials and methods

2.1. Retro-vector preparation

To construct an hCRM1 expressing retro-vector, the 3 kb fragment, which encodes the 3' part of the hCRM1 coding frame, was isolated from pSR α hCRM1 plasmid [11] by digestion with AatII and XhoI, and the left 5' part was amplified by PCR using the primer pair: hCrm15'F: CCG AAT TCT CTC TGG TAA TCT ATG CCA GCA A; hCrm15'R: CAA GTT GGG TCA GAT GAC GTC TT on pSR α hCRM1 as a template. The PCR was performed by a single step of 94 °C for 90 s and 10 cycles of a three-temperature PCR (94 °C for 30 s, 56 °C for 60 s, and 72 °C for 30 s) followed by one step of 72 °C for 5 min. The amplified fragment was then digested with AatII and EcoRI. The two fragments of hCRM1 cDNA were then ligated to retrovector pMX-neo digested with EcoRI and XhoI [40]. The resultant expression plasmid, named pMXneohCRM1, was transfected to packaging PLAT-E cells, the supernatants were collected, and stored at –80 °C.

2.2. Construction of stable cell lines

Rat mammary adenocarcinoma ER-1 cells, maintained in Dulbecco's modified Eagle's medium (DMEM, Sigma, St. Louis, MO) supplemented with 10% fetal bovine serum (FCS), were seeded into 6-well plates at a density of 1×10^5 cells/well 1 day before infection. To construct stable rat cell lines which express hCRM1, ER-1 cells were incubated with 0.5 ml of MXneohCRM1 virus solution for 4 h in the presence of 10 μ g/ml polybrene, and then fresh medium was added. The hCRM1 expressing clones were selected in the presence of 300 μ g/ml neomycin. We picked two neomycin resistant clones and designated them ER-1/hCRM1-1 and ER-1/hCRM1-2, respectively. The control cells, designated as ER-1neo1, were infected with virus carrying the MX-neo plasmid.

To construct an hCRM1 expressing rat T cell line, 1×10^5 FPM1 cells [44], an HTLV-1 transformed rat CD4⁺ T cell line, were infected with MXneohCRM1 and selected with 100 μ g/ml neomycin. The resistant cells were then divided into 96-well plates at 0.1 cells per well to clone the FPM1hCRM1-14 line.

To establish reporter cells for detection of HTLV-1-induced cell fusion, 5×10^5 293T cells in 10 cm petri dishes were transfected with 2.5 μ g of pLTR-GL3 [41] and 0.5 μ g of pTK-Hyg (Clontech, Palo Alto, CA) using Lipofectamine Plus (Invitrogen, Carlsbad, CA), according to the manufacturer's instructions. Forty-eight hours after transfection, the medium was replaced with fresh DMEM supplemented with

10% FCS and 300 µg/ml hygromycin B. Antibiotic resistant colonies were picked with a cloning cylinder. A cell clone, designated as 293T/LTR-Luc8, was used in this study.

2.3. Measurement of Rex activity

The cells (1×10^5) were transfected with 0.4 µg of pDM128RxRE [33], 0.05 µg of pSRαRex, and 0.1 µg of pCDMβ-Gal. Twenty-four hours after transfection the cells were lysed and the amount of CAT was quantified using a CAT ELISA kit (Roche). The β-galactosidase (β-gal) activity was measured by standard colorimetric methods, to normalize the transfection efficiency. The Rex activity was represented by a ratio of CAT/β-gal for each sample as described previously [33].

2.4. Measurement of HTLV-1 Gag production

The human and rat cell lines (1×10^5) were transfected with 0.5 µg of HTLV-1 infectious clone K30 and 0.1 µg of pCDMβ-Gal. Forty-eight hours after transfection, the medium of the cell culture was harvested and centrifuged at low speed to remove the cell debris. The transfected cells were washed twice with PBS then scraped off and transferred to microcentrifuge tubes; the cells were suspended in 50 µl of lysis buffer (10 mM Tris–HCl, 140 mM NaCl, 3 mM MgCl₂, 1 mM DTT, 0.5% NP-40, 1 µg/ml of aprotinin, leupeptin and pepstatin). Gag was quantified by a RETRO-TEK HTLV-1 p19 Gag ELISA kit according to the manufacturer's protocol.

2.5. Immunoblot analysis

Immunoblot analysis was performed for detection of CRM1 using affinity purified chicken anti-hCRM1 and rabbit anti-rCRM1 antibodies [33]. To detect HTLV-1 proteins, we used rabbit anti-Rex antisera, mouse anti-Tax MAb Lt-4, and mouse anti-p24 Gag MAb NOR-1 [42]. To detect the HTLV-1 Env protein, we concentrated the Env proteins using Concanavalin A (Con-A) Sepharose and then detected with rat anti-gp46 MAb LAT-27 [43]. For detection of Gag in released virions, the culture medium was ultracentrifuged at 40,000 rpm for 1 h in a Beckman TLA100.3 rotor at 4 °C. The pellets were suspended in the sample buffer and processed for immunoblotting. To detect the HTLV-1 Env protein in the cell lysate, 5×10^5 rat or human cells in 10 cm petri dishes were transfected with 2.5 µg of HTLV-1 K30. The cells were lysed 48 h after infection and applied to Con-A Sepharose. The concentrated glycoproteins were eluted using sample loading buffer.

2.6. Quantification of fusion activity of HTLV-1 infected cells

The infectious clone HTLV-1 K30 (0.5 µg) was used to transfect various rat and human cells, and 24 h later the cells were trypsinized and suspended in fresh medium. The cells were mixed with an equal number (1×10^5) of 293T/LTR₂ 1

Luc8 cells, and cultured for an additional 48 h. The cells were lysed and luciferase expression was measured using the Steady-Glo luciferase assay system (Promega, Madison, WI) to evaluate fusion activity.

2.7. Cell free infection and gene transduction analysis

The preparation of pseudotyped HTLV-1 virus and virus infection were performed, as described previously, except that the reporter plasmid, pHTC-GFP-Luc was used instead of pHTC-Luc-tsa [38]. pHTC-GFP-Luc, a newly developed reporter vector by David Derse's group, encodes a GFP-luciferase fusion protein, otherwise identical to pHTC-Luc-tsa. Briefly, pCMVHT-Δenv and pHTC-GFP-Luc, which were kindly provided by Dr David Derse, and pMD-VSV-G were transfected into 1×10^6 cells. The culture supernatant, which contains resultant viruses, was harvested 28 h after transfection and used to infect various cell types. Seventy-two hours later luciferase activity in the infected cells was measured. For AZT inhibition, 100 nM of 3'-azido-3'-deoxythymidine (AZT) (Sigma) was used to treat the infected cells as described [38].

3. Results

3.1. Effects of hCRM1 expressed in rat adenocarcinoma cell lines

We first established the stable rat adenocarcinoma cell lines, ER-1/hCRM1-1 and -2, which express hCRM1, by transduction with MxneohCRM1, a retro-vector encoding the hCRM1 cDNA. A control cell line named ER-1neo1, which carries only the neomycin resistance gene, was also generated. ER-1/hCRM1-1 and ER-1/hCRM1-2 expressed hCRM1 at levels similar to human HeLa cells and CD4-HeLa cells, as judged by immunoblotting. hCRM1 was not detected in the parental ER-1 or control ER-1neo1 cell samples (Fig. 1A). Both cell lines expressing hCRM1 propagated similarly or a little faster than parental ER-1 (Fig. 1B). It is conceivable that double the amount of CRM1 in the hCRM1 expressing rat cells, which also express rat CRM1, might facilitate rat mRNA/protein export, leading to better growth. However, it is less likely, because ER-1/neo1 grew equally well as the hCRM1 expressing ER-1 cells. In any case our results suggest that expression of physiological levels of hCRM1 does not negatively affect the replication dynamics of cells.

Next, we examined whether the hCRM1 transgene can restore Rex activity in rat cell lines. We co-transfected a CAT expressing reporter, the pDM128RxRE, pSRαRex, and pCDMβ-gal plasmids, and quantified Rex activity based on the amount of CAT protein production. In the parental rat ER-1 and control ER-1neo1 cells, Rex activity was undetectable, while in the hCRM1-expressing cells Rex activity was significantly augmented to levels found in HeLa and CD4-HeLa cells (Fig. 1C). As predicted, CAT expression in cells transfected only with pCDM128RxRE was very low. These results clearly demonstrate that expression of hCRM1 in rat cells

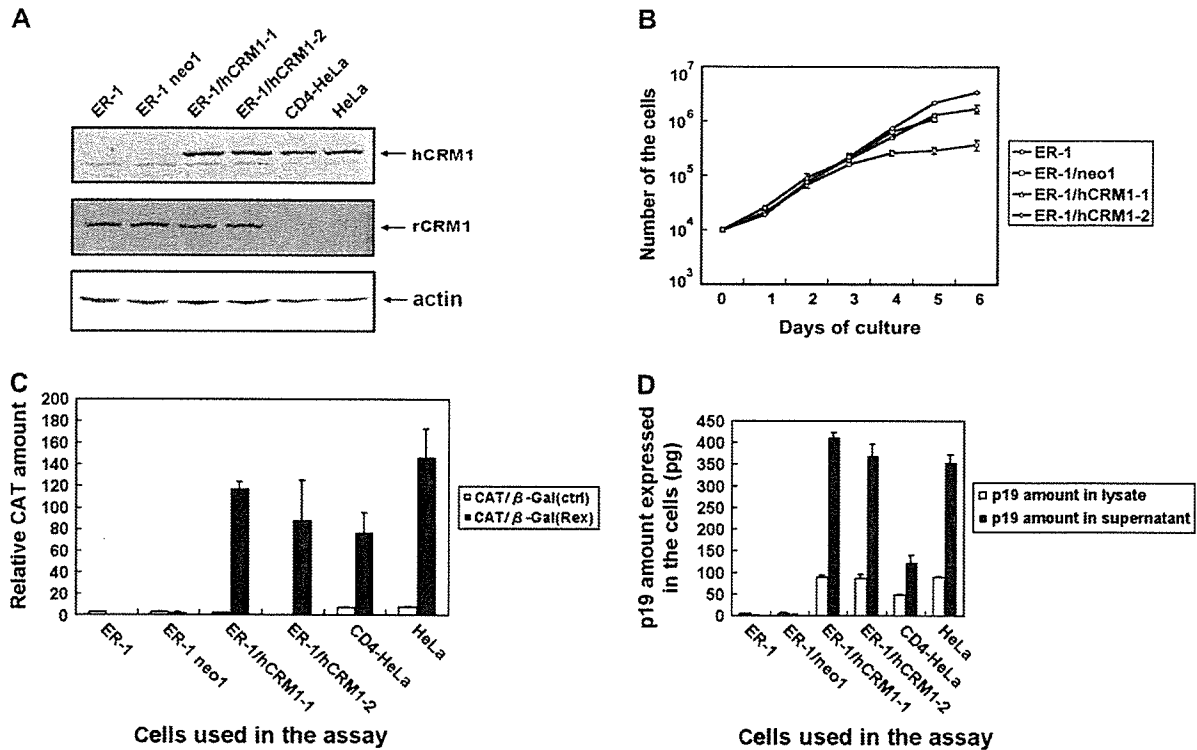


Fig. 1. Properties of hCRM1 expressing adherent rat cell lines. (A) The rat mammary tumor cell line, ER-1, was transduced with the retrovector Mx-neo-hCRM1 or Mx-neo. The expression of hCRM1 and rCRM1 in the selected clones as well as the parental rat cell and control human cell lines was examined by immunoblotting. The same amounts of the cell lysates were loaded on the SDS-PAGE. The expression of β -actin was also examined as a control to monitor the amounts of samples applied in the assay. (B) The cell growth of hCRM1-transduced rat cell clones was compared with parental ER-1. The cells (1×10^4 /ml) were seeded into a 6-well plate, and counted every 24 h. (C) hCRM1 expression enhances Rex activity in rat cells. The results are shown as the means of three independent experiments. (D) hCRM1 augments HTLV-1 Gag production in the rat cells. The rat and human cell lines were transfected with the HTLV-1 K30 and Gag products in the cell lysate and culture medium were quantified by HTLV-1 p19 ELISA. The results are shown as the mean of three independent experiments.

is sufficient to augment Rex activity to levels similar to those found endogenously in human cells, regardless of the presence of endogenous rCRM1.

The restoration of Rex activity may directly result in enhanced expression of the HTLV-1 viral structural protein. To test this possibility, we transfected rat and human cells with the HTLV-1 molecular clone K30. Gag production was first quantified using an HTLV-1 p19 antigen ELISA (Fig. 1D). The p19 antigens were produced at similar levels in hCRM1 expressing rat and human cells, whereas very low levels of p19 were detected in the parental ER-1 and control ER-1neo1 samples. The ratio of p19 in the medium to that in the cell lysate was 3–4 in both human and rat cells expressing hCRM1. Approximately 30% of the secreted Gag protein, which was produced in all types of hCRM1 expressing cells, could be pelleted by ultracentrifugation (Table 1). Taken together, these results suggest that viral particles budded from rat cells as efficiently as human cells.

To further examine the expression of the HTLV-1 structural proteins in rat cells expressing hCRM1, we performed a Western blot analysis (Fig. 2). Gag proteins including p24 and its precursor p55 were expressed equally well in human and rat cells expressing hCRM1, but were not expressed in control ER-1neo1 rat cells. The efficiency of processing p55 to p24 was similar in human and rat cells and the p38 intermediate was detected in both cell lines. Similar amounts of the HTLV-1

gp46 Env protein and its precursor gp61 were detected in both human and rat cells expressing hCRM1, but not in control ER-1neo1 rat cells. In contrast, the two trans-regulatory proteins, Tax and Rex, were expressed at similar levels in all rat and human cells upon HTLV-1 K30 transfection.

Since it is difficult to measure the infectivity of HTLV-1 by conventional methods, we applied a reporter virus assay [38], in which the HTLV-1 pseudovirus harboring a luciferase gene is coated with G proteins of vesicular stomatitis virus (VSV), which shows a broad tropism. Luciferase is driven by the

Table 1

Amount of HTLV-1 p19 Gag protein in K30-transfected rat and human cells^a

Cells	P19 amount (pg) in		
	Culture medium	Concentrated pellet	Lysate
ER-1	UD ^b	UD	UD
ER-1/neo1	UD	UD	UD
ER-1/hCRM1-1	412 ± 12	116 ± 5	89 ± 6
ER-1/hCRM1-2	369 ± 27	122 ± 9	87 ± 13
CD4-HeLa	122 ± 18	41 ± 1	48 ± 5
HeLa	355 ± 17	96 ± 2	90 ± 5

^a Cells (1×10^5) were transfected with 0.5 μ g of the HTLV-1 K30. Forty-eight hours after transfection, the cells and medium of the culture were harvested and applied to HTLV-1 p19 ELISA. The total amount of p19 was calculated. The results are shown as the mean of three independent experiments.

^b UD, under detection limit.

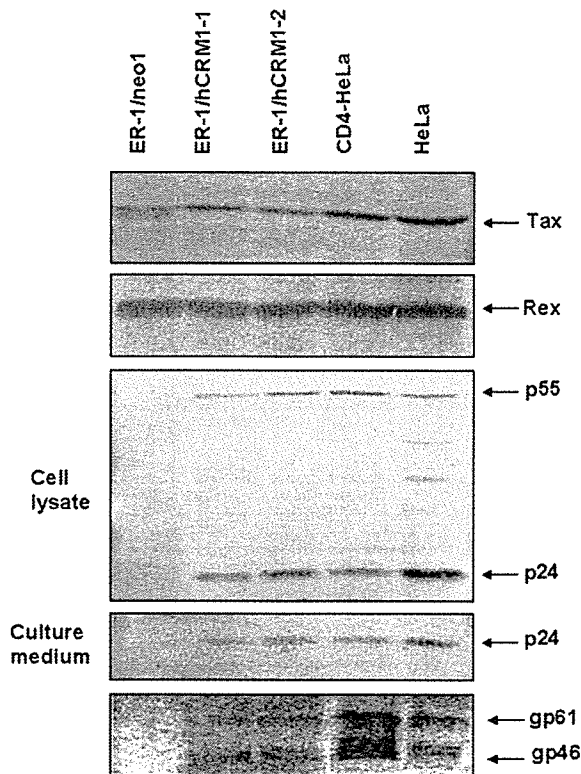


Fig. 2. hCRM1 enhances expression of HTLV-1 structural proteins, but not regulatory proteins, in rat cell lines. HTLV-1 K30-transfected cells and their culture medium were harvested and immunoblot assays were performed to detect the expression of viral proteins. The amount of samples was normalized by transfection efficiency based on β -galactosidase activity before applying to SDS-PAGE. The samples for detection of Gag in released virions and Env protein in the cell lysate were prepared as described in Section 2.

strong CMV promoter, and used as a sensitive marker of the gene expression from viral genomes, which have integrated into their host cells. We produced the pseudotyped viruses in ER-1/neo1, ER-1/hCRM1-2, HeLa and CD4-HeLa cell lines, and compared their luciferase inducing capacity after infection of 293 cells (Table 2). The pseudovirus produced in ER-1/hCRM1-2 or CD4-HeLa induced similar levels of luciferase activity, which was greater than that produced by HeLa cell derived pseudoviruses. The luciferase activity was positively correlated to the amount of HTLV-1 p19 in the medium. The luciferase activity from ER-1/neo1 samples represents the background. The luciferase activity was reduced to background levels by AZT, an inhibitor of the viral reverse transcriptase, indicating that the infection occurred through the normal retrovirus infection route. These results suggest that HTLV-1 virions produced from the hCRM1 expressing rat cells are fully infectious.

3.2. hCRM1 expression converts rat CD4⁺ T cells into high efficiency HTLV-1 producers

To examine the effect of hCRM1 expression in rat CD4⁺ T cells, we transduced MXhCRM1 into FPM1, an HTLV-1-transformed rat CD4⁺ T cell line (Fig. 3). The FPM1-derived

Table 2

Infectivity of pseudotyped HTLV-1 produced in rat and human cells^a

Cells	Luciferase activity in infected 293 cells		p19 ELISA titer (pg/ml)
	Without AZT	With AZT	
ER-1/neo1	239 ^b	261	UD
ER-1/hCRM1-2	1654	265	638
HeLa	444	132	347
CD4-HeLa	1729	370	1219

^a The pseudotyped viruses produced in various cells were quantified by p19 ELISA and infected to 293 cells in the absence or presence of AZT. Seventy-two hours later luciferase activity in the infected cells was measured. Representative results of two independent experiments are shown.

^b RLU, relative light units.

hCRM1 expressing cells, FPM1-hCRM1-14, produced hCRM1 levels comparable to the Jurkat human T cell line and to MT-4, an HTLV-1 producing human T cell line. FPM1-hCRM1-14 grew as well as the parental FPM1 cells (Fig. 3A). FPM1 has been reported to selectively express viral regulatory proteins, such as Tax, but not structural proteins [44]. Our ELISA data consistently showed very low levels of p19 expression (approximately 25 pg/ml) in the culture medium of FPM1, whereas FPM1-hCRM1-14 produced very high levels of secreted Gag antigen (approximately 7400 pg/ml), comparable to MT-4 cells (data not shown).

Western blotting showed that expression of hCRM1 in FPM1 did not affect the amount of Tax and Rex proteins, which are encoded by mRNAs that are exported independently of CRM1. In contrast, hCRM1 augmented the production of Gag and Env proteins. The Gag precursor p55 was processed to mature p24 as efficiently as the human T cells (Fig. 3B).

3.3. Fusion ability of HTLV-1-infected rat cells

Efficient spread of HTLV-1 requires cell contact [45,46]. Lymphocytes naturally infected with HTLV-1 produce very few cell-free HTLV-1 virions, and one in 10⁵ to 10⁶ virions is estimated to be infectious [38,39]. The cell-to-cell spread of HTLV-1 is mediated through fusion of the two cell membranes caused by Env proteins [23,47,48]. Certain integrins, including the intercellular and vascular cell adhesion molecules ICAM-1, ICAM-3, and VCAM, act as cofactors for HTLV-1-induced cell fusion [49,50]. To quantify the fusion efficiency of HTLV-1-infected cells, we established a 293T derived reporter cell, 293/LTR-luc8, which harbors an HTLV-1 LTR promoter-driven luciferase reporter gene. When cell fusion occurs following co-culture of this reporter cell with HTLV-1 producing cells, Tax protein is transferred from the donor cells and activates the LTR promoter. An alternative route to activate the luciferase gene is through newly synthesized Tax protein from an HTLV-1 genome, which has been transferred from the donor cells, reverse-transcribed, and integrated into a reporter cell chromosome. In either case, the fusion ability of the HTLV-1 infected cells can be evaluated by luciferase expression. The reporter cells express very low levels of luciferase under normal culture conditions,

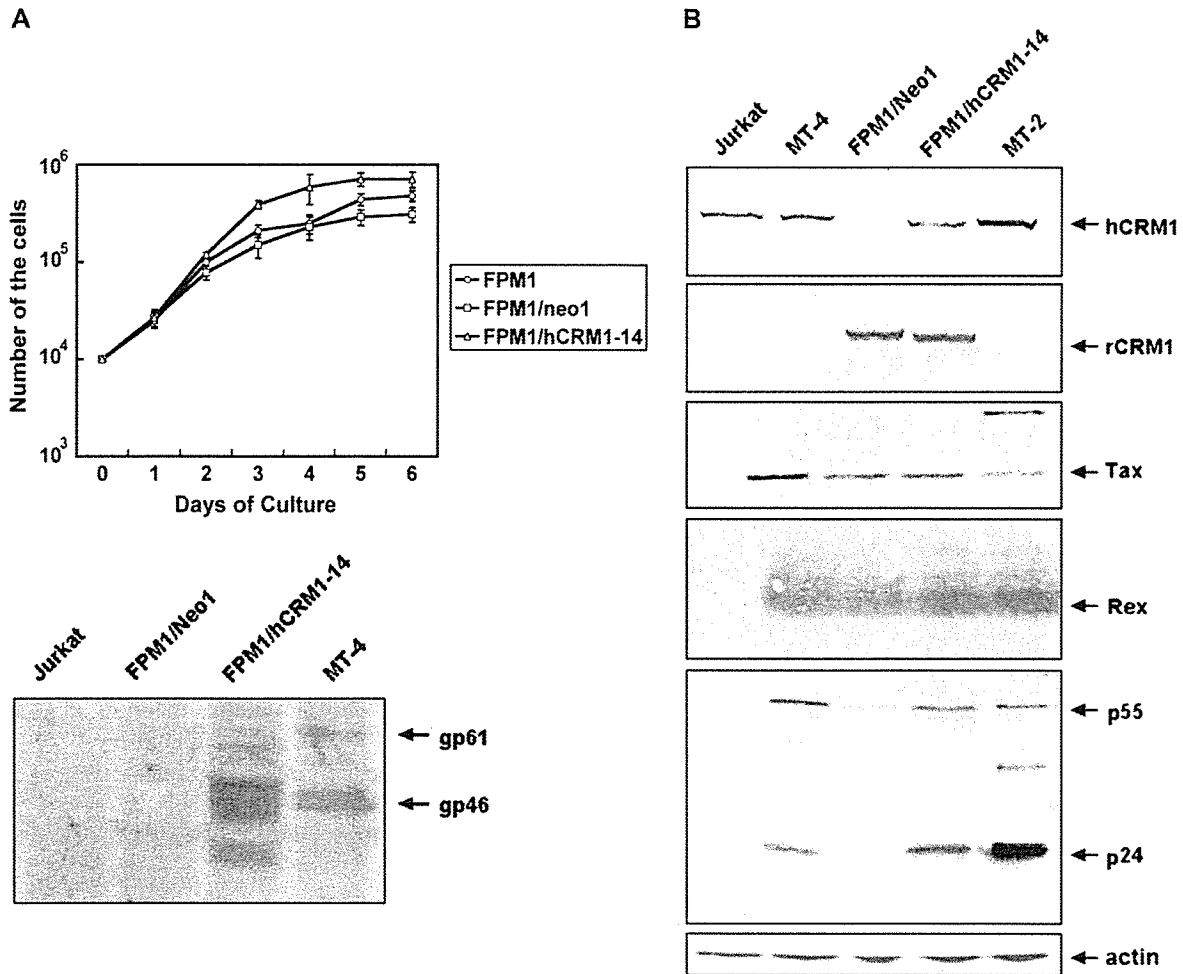


Fig. 3. hCRM1 enhanced viral structural protein expression in HTLV-1-infected rat T-cell lines. (A) The cell growth of hCRM1-transduced rat T cell clones was compared with parental FPM1 cells. The cells (1×10^4 /ml) were seeded into a 6-well plate, and counted every 24 h. (B) HTLV-1-infected and uninfected rat and human T cells (1×10^6 cells) were harvested in their log growth phase. Immunoblotting was performed as in Fig. 1A and Fig. 2. The expression of β -actin was also examined as a control to monitor the amounts of samples applied in the assay.

but have a very sensitive LTR response upon Tax stimulation, as demonstrated by transient expression of a Tax encoding plasmid (data not shown), or co-culture with as few as 1×10^3 HTLV-1 producing MT-2 cells. Luciferase activity increased linearly with the number of MT-2 cells, up to 5×10^4 cells. In contrast, co-culture with 5×10^4 Jurkat cells did not induce luciferase activity (Fig. 4A).

To compare the fusion capability of virus-producing cells, we first transfected various rat and human cells with HTLV-1 K30, incubated the cells for 24 h after transfection, and then co-cultured them with 293T/LTR-luc8 cells for a further 72 h. As shown in Fig. 4B, the luciferase activity induced by co-culture with ER-1/hCRM1-1 and ER-1/hCRM1-2 was as high as that resulting from co-culture with HeLa or CD4-HeLa cells, as well as the HTLV-1 high producing line C77, suggesting that K30-infected rat cells could be highly infectious. In contrast, the luciferase expression in reporter cells co-cultured with ER-1neo1 was close to the basal level. As a control, rat and human cells transfected with a Tax expressing plasmid pSR α Tax in the absence of Env expression were also unable to increase luciferase expression when co-cultured

with 293T/LTR-luc8 cells (data not shown), indicating that luciferase expression depends on cell fusion mediated by Env proteins.

The fusion ability of HTLV-1-infected rat T cells was also investigated. The luciferase level in reporter cells co-cultured with both human T cells (MT-4) and FPM1-mxhCRM1-14 were unexpectedly lower than the adherent cells described above. Nevertheless, the hCRM1 expressing rat T cells stimulated luciferase activity more efficiently than MT-4 cells (Fig. 4C). Luciferase activity was proportional to the amount of Env gp46 expressed (see Figs. 3 and 4). These results clearly demonstrate that the Env protein induced by hCRM1 in the rat cells is fully fusogenic, supporting HTLV-1 infectivity in rat cells.

To discriminate whether a Tax protein transferred from the donor cells or Tax protein produced from the HTLV-1 genome which had infected the reporter cells was the primary inducer of luciferase, we co-cultured the infected and reporter cells in the presence of AZT. The former alternative would be insensitive to AZT, while the latter would be sensitive to AZT. AZT at 100 nM had a negligible effect on luciferase activity (data not

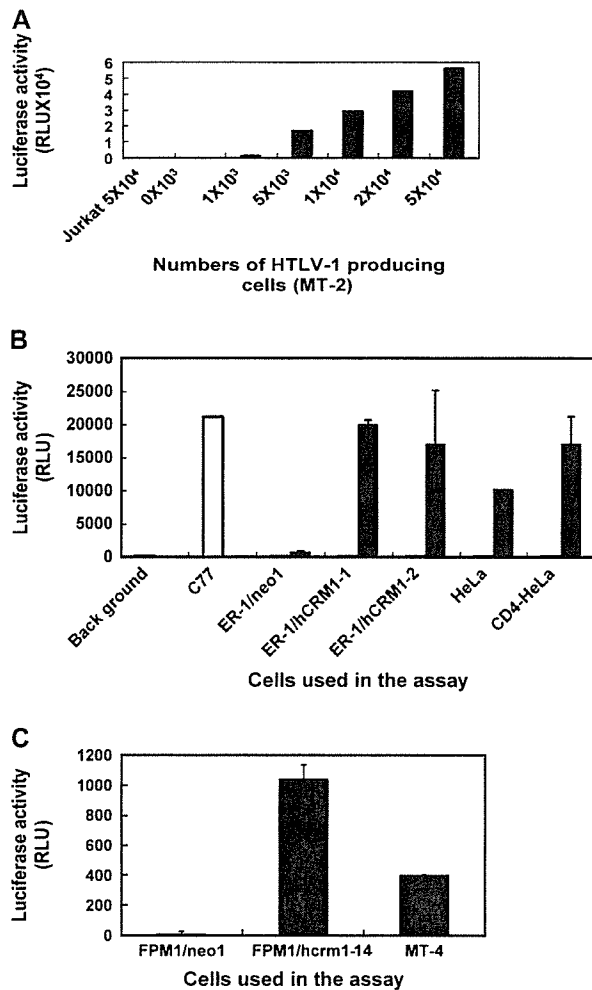


Fig. 4. Env proteins expressed in the rat cells are fusogenic. (A) Various numbers of MT-2 cells were co-cultured with 1×10^5 of the reporter cell 293T/LTR-Luc8. One-fourth of the cell lysate was for the luciferase assay. RLU, relative light units. (B) Luciferase activity induced in reporter cells co-cultured with the HTLV-1 K30-transfected rat and human cells. The results are shown as the mean of three independent experiments. (C) Luciferase activity in the reporter cells co-cultured with HTLV-1 producing rat and human T cells. The results are shown as the mean of two independent experiments.

shown), consistent with poor formation of HTLV-1 infectious virus.

3.4. Efficient early events of HTLV-1 replication in rat cells

To determine the efficiency of early replication events, from entry to the genome integration step, human and rat cells were infected with VSV G-pseudotyped HTLV-1 virus containing the GFP-luciferase gene. ER-1/neo1 and ER1/hCRM1-2 cells produced luciferase signals similar to 293 and 293T cells (Table 3, Experiment 1). Unexpectedly, HeLa and CD4-HeLa cells produced much weaker signals. Luciferase activity was inhibited by the reverse transcriptase inhibitor AZT, indicating that luciferase expression occurred as a result of retrovirus replication, implying reverse-transcription and integration. We next compared the efficiency of the early events

Table 3

Transduction efficiencies of pseudotyped HTLV-1 to various cells

Cells	Luciferase activity (RLU)	
	Without AZT	With AZT
<i>Experiment 1^a</i>		
ER-1/neo1	3320	228
ER-1/hCRM1-2	2798	126
HeLa	98	103
CD4-HeLa	175	308
293	1946	197
293T	4485	293
<i>Experiment 2^b</i>		
FPM1	995	275
FPM1/hCRM1-14	465	132
Nb2	860	156
MT-4	2908	416
Jurkat	758	307
Molt-4	884	300

^a Filtered supernatant of 293T cotransfected with pCMVHT-Δenv, pHTC-GFP-Luc, and pMD-VSV-G were applied to infect 1×10^5 adherent cells. The p19 in the supernatant was 19 ng/ml. Representative results of two independent experiments are shown.

^b The filtered supernatant was ultra-centrifuged at 14,000 rpm for 90 min. The pellet resultant was suspended in 100 μl of fresh medium, and used to infect the rat and human cells.

in rat T cells with those in human T cells. As shown in Table 3 Experiment 2, both HTLV-1-uninfected (Nb2) and infected rat T cells (FPM1) induced luciferase as much as the human T cells. These results suggest that the early events of HTLV-1 infection indeed occurred in the rat cells at the same or slightly higher levels than in human cells. Free HTLV-1 viruses prepared from feline HTLV-1 producing C77 cells were used to infect activated primary T cells prepared from human PBMC or rat spleen. PCR was used to detect the pX region of HTLV-1 in genomic DNA, extracted from the cells 3 days after infection. We found more intensive signals in the rat T cell samples than the human samples (data not shown). This result supports the above notion, although it is not a quantitative method.

4. Discussion

Previously, we have shown that rCRM1, even though it is able to export Rex protein from the nucleus, does not support Rex multimerization, resulting in poor export of HTLV-1 RNAs in rat cells [33,34]. In this study, we demonstrated that the expression of hCRM1 at physiological levels in rat cells, including epithelial and CD4⁺ T cells, is not harmful to cell growth, but augments the synthesis of HTLV-1 Gag and Env proteins to levels similar to those seen in human cells. The endogenous rCRM1 does not inhibit the function of Rex, although rCRM1 overexpressed by transfection has been reported to act as a dominant negative inhibitor of hCRM1 function [33]. The Gag precursor synthesized in hCRM1 expressing rat cells is normally processed to the mature p24 and possibly other Gag proteins and then released into the culture medium as sedimentable viral particles, with

an efficiency comparable to human cell lines. The fact that only 25–30% of the Gag protein detected in the medium of both human and rat cells was sedimentable suggests that only a fraction of the Gag proteins may be incorporated into virions, or that the non-sedimentable Gag proteins may reflect the fragility of the virus. Finally, the results using the HTLV-1 pseudovirus [38] suggest that HTLV-1 virions released from the rat cells may have the same infectivity as those released from human cells.

A major route for the spread of HTLV-1 is cell to cell infection mediated by cell fusion caused by the Env proteins in cooperation with the cell adhesion molecules ICAM-1, ICAM-3, and VCAM [48,49]. Some reports suggest that the main function of the Env protein is to mediate cell fusion. These data led us to develop a reporter cell line to quantify Env-mediated cell fusion, based on activation of an HTLV-1 LTR-driven luciferase gene. This system can detect fusion events between as little as approximately 1×10^3 MT-2 cells and 1×10^4 K30-infected cells. Given that this fusion has been shown to be dependent on the Env protein, quantitation of functional Env proteins by this system should be much more sensitive than Western blotting, which requires Env protein concentrated by Con A Sepharose from at least 5×10^5 K30-infected cells. Using this system, we demonstrated that hCRM1 expressing rat cells infected with HTLV-1 mediate cell fusion as efficiently as human cell lines. The results suggest that the fusion capacity of human and rat cells is proportional to the amount of the Env gp46 protein detected by Western blotting (compare Figs. 2, 3 and 4), and indicates that the Env expressed on rat cells is fully fusogenic, which is the basis for HTLV-1 cell to cell transmission.

The poor replication of HTLV-1 in rat cells is unlikely to be related to efficiency of viral entry, since HTLV-1 has a broad host range of infection using Env-coated virus systems [29–31]. The results of our cell fusion-dependent reporter assay (Fig. 4) are consistent with these observations and with the data suggesting that the ubiquitously expressed Glut-1 acts as a HTLV-1 receptor [32]. The post entry steps, including reverse-transcription, nuclear entry, and integration of the HTLV-1 genome, should not be severely inhibited in rat cells since our results using the HTLV-1 pseudovirus system [9] indicate that the infected rat cells induced luciferase, a quantitative marker for successful integration of the viral genome, at levels similar to human cells. Moreover, the early viral proteins, such as Tax and Rex, which are expressed independently of Rex function, are efficiently synthesized in rat cells (Figs. 2 and 3) [44]. Our results suggest that rat cells do not have serious blockages in viral replication other than rCRM1 in the late stage.

In conclusion, rCRM1 can be considered a major species-specific barrier for HTLV-1 replication in rat cells. This barrier is unique to HTLV-1, since, for many viruses, this restriction is determined by species-specific receptor interactions. The fact that expression of hCRM1 allows rat cells to produce high amounts of fully functional Gag and Env proteins and assemble infectious HTLV-1 suggests the feasibility of constructing a transgenic rat expressing hCRM1, which could present

a better animal model to study HTLV-1 infection and develop preventive and therapeutic intervention strategies.

Acknowledgements

We thank the NIH AIDS research and reference reagent program for providing HTLV-1 K30, Dr David Derse for the gift of pCMVHT-Δ Env and pHTC-GFP-Luc, Dr. Mari Kannagi for FPM1 and Dr Jun-ichi Fujisawa for providing pLTR-GL3.

References

- [1] Y. Hinuma, K. Nagata, M. Hanaoka, M. Nakai, T. Matsumoto, K.I. Kinoshita, S. Shirakawa, I. Miyoshi, Adult T-cell leukemia: antigen in an ATL cell line and detection of antibodies to the antigen in human sera, *Proc. Natl. Acad. Sci. U.S.A.* 78 (1981) 6476–6480.
- [2] M. Osame, K. Usuku, S. Izumo, N. Ijichi, H. Amitani, A. Igata, M. Matsumoto, M. Tara, HTLV-I associated myelopathy, a new clinical entity, *Lancet* 1 (1986) 1031–1032.
- [3] G. Franchini, Molecular mechanisms of human T-cell leukemia/lymphotropic virus type I infection, *Blood* 86 (1995) 3619–3639.
- [4] M. Yoshida, Multiple viral strategies of HTLV-1 for dysregulation of cell growth control, *Annu. Rev. Immunol.* 19 (2001) 475–496.
- [5] M. Hidaka, J. Inoue, M. Yoshida, M. Seiki, Post-transcriptional regulator (rex) of HTLV-1 initiates expression of viral structural proteins but suppresses expression of regulatory proteins, *EMBO J.* 7 (1988) 519–523.
- [6] B.R. Cullen, Regulation of human immunodeficiency virus replication, *Annu. Rev. Microbiol.* 45 (1991) 219–250.
- [7] J. Inoue, M. Yoshida, M. Seiki, Transcriptional (p40x) and post-transcriptional (p27x-III) regulators are required for the expression and replication of human T-cell leukemia virus type I genes, *Proc. Natl. Acad. Sci. U.S.A.* 84 (1987) 3653–3657.
- [8] C. Ballaun, G.K. Farrington, M. Dobrovnik, J. Rusche, J. Hauber, E. Bohlslein, Functional analysis of human T-cell leukemia virus type I rex-response element: direct RNA binding of Rex protein correlates with *in vivo* activity, *J. Virol.* 65 (1991) 4408–4413.
- [9] H.P. Bogerd, G.L. Huckaby, Y.F. Ahmed, S.M. Hanly, W.C. Greene, The type I human T-cell leukemia virus (HTLV-I) Rex trans-activator binds directly to the HTLV-I Rex and the type I human immunodeficiency virus Rev RNA response elements, *Proc. Natl. Acad. Sci. U.S.A.* 88 (1991) 5704–5708.
- [10] M. Fomerod, M. Ohno, M. Yoshida, I.W. Mattaj, CRM1 is an export receptor for leucine-rich nuclear export signals, *Cell* 90 (1997) 1051–1060.
- [11] Y. Hakata, T. Umemoto, S. Matsushita, H. Shida, Involvement of human CRM1 (exportin 1) in the export and multimerization of the Rex protein of human T-cell leukemia virus type 1, *J. Virol.* 72 (1998) 6602–6607.
- [12] M.E. Nemergut, M.E. Lindsay, A.M. Brownawell, I.G. Macara, Ran-binding protein 3 links Crm1 to the Ran guanine nucleotide exchange factor, *J. Biol. Chem.* 277 (2002) 17385–17388.
- [13] H. Bogerd, W.C. Greene, Dominant negative mutants of human T-cell leukemia virus type I Rex and human immunodeficiency virus type I Rev fail to multimerize *in vivo*, *J. Virol.* 67 (1993) 2496–2502.
- [14] H. Shida, Y. Hakata, Multiple roles of cellular export machinery in HTLV-1 Rex functioning, *Gann monogr.* 50 (2003) 61–72.
- [15] H. Shida, T. Tochikura, T. Sato, T. Konno, K. Hirayoshi, M. Seki, Y. Ito, M. Hatanaka, Y. Hinuma, M. Sugimoto, et al., Effect of the recombinant vaccinia viruses that express HTLV-I envelope gene on HTLV-1 infection, *EMBO J.* 6 (1987) 3379–3384.
- [16] K. Ogawa, S. Matsuda, A. Seto, Induction of leukemic infiltration by allogeneic transfer of HTLV-I-transformed T cells in rabbits, *Leuk. Res.* 13 (1989) 399–406.
- [17] Y. Tanaka, R. Tanaka, E. Terada, Y. Koyanagi, N. Miyano-Kurosaki, N. Yamamoto, E. Baba, M. Nakamura, H. Shida, Induction of antibody responses that neutralize human T-cell leukemia virus type I infection

- in vitro and in vivo by peptide immunization, *J. Virol.* 68 (1994) 6323–6331.
- [18] M. Kazanji, A. Ureta-Vidal, S. Ozden, F. Tangy, B. de Thoisy, L. Fiette, A. Talarmin, A. Gessain, G. de Thé, The Lymphoid organs as a major reservoir for human T-cell leukemia virus type I in experimentally infected squirrel monkeys (*Saimiri sciureus*): provirus expression, persistence, and humoral and cellular immune responses, *J. Virol.* 74 (2000) 4860–4867.
- [19] T.M. McGinn, Q. Wei, J. Stallworth, P.N. Fultz, Immune responses to HTLV-I(ACH) during acute infection of pig-tailed macaques, *AIDS Res. Hum. Retroviruses* 20 (2004) 443–456.
- [20] K. Ibuki, S.I. Funahashi, H. Yamamoto, M. Nakamura, T. Igarashi, T. Miura, E. Ido, M. Hayami, H. Shida, Long-term persistence of protective immunity in cynomolgus monkeys immunized with a recombinant vaccinia virus expressing the human T cell leukaemia virus type I envelope gene, *J. Gen. Virol.* 78 (Pt 1) (1997) 147–152.
- [21] R. Feng, A. Kabayama, K. Uchida, H. Hoshino, M. Miwa, Cell-free entry of human T-cell leukemia virus type I to mouse cells, *Jpn. J. Cancer Res.* 92 (2001) 410–416.
- [22] C. Denesvre, P. Sonigo, A. Corbin, H. Ellerbrok, M. Sitbon, Influence of transmembrane domains on the fusogenic abilities of human and murine leukemia retrovirus envelopes, *J. Virol.* 69 (1995) 4149–4157.
- [23] K. Nagy, P. Clapham, R. Cheingsong-Popov, R.A. Weiss, Human T-cell leukemia virus type I: induction of syncytia and inhibition by patients' sera, *Int. J. Cancer* 32 (1983) 321–328.
- [24] B. Sun, T. Nitta, M. Shoda, M. Tanaka, S. Hanai, H. Hoshino, M. Miwa, Cell-free human T-cell leukemia virus type I binds to, and efficiently enters mouse cells, *Jpn. J. Cancer Res.* 93 (2002) 760–766.
- [25] F. Ibrahim, L. Fiette, A. Gessain, N. Buisson, G. de-Thé, R. Bomford, Infection of rats with human T-cell leukemia virus type-I: susceptibility of inbred strains, antibody response and provirus location, *Int. J. Cancer* 58 (1994) 446–451.
- [26] T. Suga, T. Kameyama, T. Kinoshita, K. Shimotohno, M. Matsumura, H. Tanaka, S. Kushida, Y. Ami, M. Uchida, K. Uchida, et al., Infection of rats with HTLV-I: a small-animal model for HTLV-I carriers, *Int. J. Cancer* 49 (1991) 764–769.
- [27] N. Ishiguro, M. Abe, K. Seto, H. Sakurai, H. Ikeda, A. Wakisaka, T. Togashi, M. Tateno, T. Yoshiki, A rat model of human T lymphocyte virus type I (HTLV-I) infection. I. Humoral antibody response, provirus integration, and HTLV-I-associated myelopathy/tropical spastic paraparesis-like myelopathy in seronegative HTLV-I carrier rats, *J. Exp. Med.* 176 (1992) 981–989.
- [28] T. Kasai, H. Ikeda, U. Tomaru, I. Yamashita, O. Ohya, K. Morita, A. Wakisaka, E. Matsuoka, T. Moritoyo, K. Hashimoto, I. Higuchi, S. Izumo, M. Osame, T. Yoshiki, A rat model of human T lymphocyte virus type I (HTLV-I) infection: in situ detection of HTLV-I provirus DNA in microglia/macrophages in affected spinal cords of rats with HTLV-I-induced chronic progressive myeloneuropathy, *Acta. Neuropathol. (Berl)* 97 (1999) 107–112.
- [29] Q.X. Li, D. Camerini, Y. Xie, M. Greenwald, D.R. Kuritzkes, I.S. Chen, Syncytium formation by recombinant HTLV-II envelope glycoprotein, *Virology* 218 (1996) 279–284.
- [30] R.E. Sutton, D.R. Littman, Broad host range of human T-cell leukemia virus type I demonstrated with an improved pseudotyping system, *J. Virol.* 70 (1996) 7322–7326.
- [31] K. Okuma, M. Nakamura, S. Nakano, Y. Niho, Y. Matsuura, Host range of human T-cell leukemia virus type I analyzed by a cell fusion-dependent reporter gene activation assay, *Virology* 254 (1999) 235–244.
- [32] N. Manel, F.J. Kim, S. Kinet, N. Taylor, M. Sitbon, J.L. Battini, The ubiquitous glucose transporter GLUT-1 is a receptor for HTLV, *Cell* 115 (2003) 449–459.
- [33] Y. Hakata, M. Yamada, H. Shida, Rat CRM1 is responsible for the poor activity of human T-cell leukemia virus type I Rex protein in rat cells, *J. Virol.* 75 (2001) 11515–11525.
- [34] Y. Hakata, M. Yamada, H. Shida, A multifunctional domain in human CRM1 (exportin 1) mediates RanBP3 binding and multimerization of human T-cell leukemia virus type I Rex protein, *Mol. Cell. Biol.* 2 (2003) 8751–8761.
- [35] M. Callanan, N. Kudo, S. Gout, M. Brocard, M. Yoshida, S. Dimitrov, S. Khochbin, Developmentally regulated activity of CRM1/XPO1 during early *Xenopus* embryogenesis, *J. Cell Sci.* 113 (Pt 3) (2000) 451–459.
- [36] M. Stremlau, C.M. Owens, M.J. Perron, M. Kiessling, P. Autissier, J. Sodroski, The cytoplasmic body component TRIM5 α restricts HIV-1 infection in Old World monkeys, *Nature* 427 (2004) 848–853.
- [37] A.M. Sheehy, N.C. Gaddis, J.D. Choi, M.H. Malim, Isolation of a human gene that inhibits HIV-1 infection and is suppressed by the viral Vif protein, *Nature* 418 (2002) 646–650.
- [38] D. Derse, S.A. Hill, P.A. Lloyd, H. Chung, B.A. Morse, Examining human T-lymphotropic virus type I infection and replication by cell-free infection with recombinant virus vectors, *J. Virol.* 75 (2001) 8461–8468.
- [39] N. Fan, J. Gavalchin, B. Paul, K.H. Wells, M.J. Lane, B.J. Poiesz, Infection of peripheral blood mononuclear cells and cell lines by cell-free human T-cell lymphoma/leukemia virus type I, *J. Clin. Microbiol.* 30 (1992) 905–910.
- [40] M. Onishi, S. Kinoshita, Y. Morikawa, A. Shibuya, J. Phillips, L.L. Lanier, D.M. Gorman, G.P. Nolan, A. Miyajima, T. Kitamura, Application of retrovirus-mediated expression cloning, *Exp. Hematol.* 24 (1996) 324–329.
- [41] J. Fujisawa, M. Seiki, T. Kiyokawa, M. Yoshida, Functional activation of the long terminal repeat of human T-cell leukemia virus type I by a trans-acting factor, *Proc. Natl. Acad. Sci. U.S.A.* 82 (1985) 2277–2281.
- [42] Y. Tanaka, M. Yasumoto, H. Nyunoya, T. Ogura, M. Kikuchi, K. Shimotohno, H. Shiraki, N. Kuroda, H. Shida, H. Tozawa, Generation and characterization of monoclonal antibodies against multiple epitopes on the C-terminal half of envelope gp46 of human T-cell leukemia virus type-I (HTLV-I), *Int. J. Cancer* 46 (1990) 675–681.
- [43] Y. Tanaka, L. Zeng, H. Shiraki, H. Shida, H. Tozawa, Identification of a neutralization epitope on the envelope gp46 antigen of human T cell leukemia virus type I and induction of neutralizing antibody by peptide immunization, *J. Immunol.* 147 (1991) 354–360.
- [44] Y. Koya, T. Ohashi, H. Kato, S. Hanabuchi, T. Tsukahara, F. Takemura, K. Etoh, M. Matsuoka, M. Fujii, M. Kannagi, Establishment of a seronegative human T-cell leukemia virus type I (HTLV-I) carrier state in rats inoculated with a syngeneic HTLV-I-immortalized T-cell line preferentially expressing Tax, *J. Virol.* 73 (1999) 6436–6443.
- [45] N. Yamamoto, M. Okada, Y. Koyanagi, M. Kannagi, Y. Hinuma, Transformation of human leukocytes by cocultivation with an adult T cell leukemia Virus producer cell line, *Science* 217 (1982) 737–739.
- [46] M. Popovic, P.S. Sarin, M. Robert-Gurroff, V.S. Kalyanaraman, D. Mann, J. Minowada, R.C. Gallo, Isolation and transmission of human retrovirus (human t-cell leukemia virus), *Science* 219 (1983) 856–859.
- [47] L. Delamarre, A.R. Rosenberg, C. Pique, D. Pham, M.C. Dokhelar, A novel human T-leukemia virus type I cell-to-cell transmission assay permits definition of SU glycoprotein amino acids important for infectivity, *J. Virol.* 71 (1997) 259–266.
- [48] S.R. Jassal, M.D. Lairmore, A.J. Leigh-Brown, D.W. Brighty, Soluble recombinant HTLV-1 surface glycoprotein competitively inhibits syncytia formation and viral infection of cells, *Virus. Res.* 78 (2001) 17–34.
- [49] J.E. Hildreth, A. Subramaniam, R.A. Hampton, Human T-cell lymphotropic virus type I (HTLV-I)-induced syncytium formation mediated by vascular cell adhesion molecule-1: evidence for involvement of cell adhesion molecules in HTLV-1 biology, *J. Virol.* 71 (1997) 1173–1180.
- [50] S. Daenke, S.A. McCracken, S. Booth, Human T-cell leukaemia/lymphoma virus type I syncytium formation is regulated in a cell-specific manner by ICAM-1, ICAM-3 and VCAM-1 and can be inhibited by antibodies to integrin β 2 or β 7, *J. Gen. Virol.* 80 (Pt 6) (1991) 429–436.

Anti-V3 Humanized Antibody KD-247 Effectively Suppresses Ex Vivo Generation of Human Immunodeficiency Virus Type 1 and Affords Sterile Protection of Monkeys against a Heterologous Simian/Human Immunodeficiency Virus Infection

Yasuyuki Eda,¹ Toshio Murakami,¹ Yasushi Ami,² Tadashi Nakasone,³ Mari Takizawa,³ Kenji Someya,³ Masahiko Kaizu,³ Yasuyuki Izumi,³ Naoto Yoshino,³ Shuzo Matsushita,⁴ Hirofumi Higuchi,¹ Hajime Matsui,¹ Katsuaki Shinohara,⁵ Hiroaki Takeuchi,⁶ Yoshio Koyanagi,⁶ Naoki Yamamoto,³ and Mitsuo Honda^{3*}

The Chemo-Sero-Therapeutic Research Institute, Kyokushi, Kikuchi, Kumamoto 869-1298, Japan¹; Division of Experimental Animal Research,² AIDS Research Center,³ and Division of Biosafety Control,⁵ Department of Safety Research on Biologics, National Institute of Infectious Diseases, Shinjuku-ku, Tokyo 162-8640, Japan; Center for AIDS Research, Kumamoto University, Kumamoto 860-0811, Japan⁴; and Institute of Viral Research, Kyoto University, Kyoto 606-8507, Japan⁶

Received 5 October 2005/Accepted 9 March 2006

In an accompanying report (Y. Eda, M. Takizawa, T. Murakami, H. Maeda, K. Kimachi, H. Yonemura, S. Koyanagi, K. Shiosaki, H. Higuchi, K. Makizumi, T. Nakashima, K. Osatomi, S. Tokiyoshi, S. Matsushita, N. Yamamoto, and M. Honda, *J. Virol.* 80:5552-5562, 2006), we discuss our production of a high-affinity humanized monoclonal antibody, KD-247, by sequential immunization with V3 peptides derived from human immunodeficiency virus type 1 (HIV-1) clade B primary isolates. Epitope mapping revealed that KD-247 recognized the Pro-Gly-Arg V3 tip sequence conserved in HIV-1 clade B isolates. In this study, we further demonstrate that in vitro, KD-247 efficiently neutralizes CXCR4- and CCR5-tropic primary HIV-1 clade B and clade B' with matching neutralization sequence motifs but does not neutralize sequence-mismatched clade B and clade E isolates. Monkeys were provided sterile protection against heterologous simian/human immunodeficiency virus challenge by the passive transfer of a single high dose (45 mg per kg of body weight) of KD-247 and afforded partial protection by lower antibody doses (30 and 15 mg per kg). Protective neutralization endpoint titers in plasma at the time of virus challenge were 1:160 in animals passively transferred with a high dose of the antibody. The antiviral efficacy of the antibody was further confirmed by its suppression of the ex vivo generation of primary HIV-1 quasispecies in peripheral blood mononuclear cell cultures from HIV-infected individuals. Therefore, KD-247 promises to be a valuable tool not only as a passive immunization antibody for the prevention of HIV infection but also as an immunotherapy for the suppression of HIV in phenotype-matched HIV-infected individuals.

Because most primary strains of human immunodeficiency virus type 1 (HIV-1) are relatively resistant to neutralization, the specificities of antibodies that confer protective immunity against it are still not understood (22). Previously, we and others (9, 31) have reported that chimpanzees can be protected against infection with the T-cell-line-adapted strain HIV-1_{IIB} by passive transfer of either HIV immunoglobulin (Ig) (HIVIG) or anti-HIV-1_{IIB} V3 monoclonal antibodies (MAbs). Passive administration of the anti-HIV-1 gp41 human MAb 2F5 (24) to two chimpanzees prior to challenge with primary HIV-1₅₀₁₆ resulted in a delay in plasma viremia and reduced viral load. Since the chimpanzee model is limited by the failure of HIV-1 to induce disease in these animals, a pathogenic model was developed in monkeys using a simian/human immunodeficiency virus (SHIV) strain that is capable of inducing high plasma viremia, CD4⁺-T-cell loss, and simian AIDS (11, 14,

15, 37). Following pathogenic SHIV 89.6P challenge, Mascola and colleagues (20) previously noted a synergistic effect with the passively transferred antibody HIVIG, a MAb against membrane-proximal external region 2F5 (27), and 2G12, a glycan-dependent MAb (41). Monkeys were afforded protective immunity against pathogenic SHIV DH12 by chimpanzee HIVIG and provided sterile protection against the challenge virus when given high-dose inoculations (27, 36). However, sterile protection was strain specific, and the antiserum did not bind a V3 loop peptide or block the interaction of gp120 with CD4. In several passive immunization studies using MAbs, the antibodies 2G12 and 2F5 as well as 4410, a MAb against membrane-proximal external region 4E10 (4), have been shown to inhibit SHIV in monkeys (2, 20, 21). Furthermore, human MAb b12, targeting the CD4-binding domain of gp120, has been reported to elicit complete protection against viral challenge (29) and partial protection against MAb 2G12 (22) in monkeys. Recently, passively transferred antibodies with 2G12, 2F5, and 4E10 were shown to delay the rebound of HIV-1 after the cessation of antiretroviral therapy, with that delay especially pronounced in acutely infected individuals.

* Corresponding author. Mailing address: AIDS Research Center, National Institute of Infectious Diseases, Shinjuku-ku, Tokyo 162-8640, Japan. Phone: 81-3-5285-1111, ext. 2737. Fax: 81-3-5285-1183. E-mail: mhonda@nih.go.jp.

The *in vivo* effect of the neutralizing antibody cocktail was found to depend on 2G12 activity by escape mutant analysis (42).

It has been established that anti-V3 antibodies, induced by brief immunization protocols in animals, are capable of neutralizing HIV-1 in cell cultures and in animal challenge studies (13, 16, 27, 28). However, that capability has not been fully exploited because the V3 sequence is extremely diverse, and so the anti-V3 antibodies are extremely type specific and displayed little cross-reactivity. In the accompanying paper (8a), we describe how we sequentially immunized mice with V3 peptides derived from several different HIV-1 clade B field isolates. The antibody response could be traced to a tip sequence of the HIV-1 gp120 V3 domain, a relatively conserved motif (11, 18, 45). We reshaped anti-V3 MAb C25 into KD-247, a humanized MAb directed against the V3 tip motif Pro-Gly-Arg of the V3 domain. KD-247 cross-neutralized primary isolates with a matching neutralization sequence motif, suggesting that it could be used to overcome the previous limitations surrounding anti-V3 neutralizing antibody production by active immunization strategies.

In this study, we show that the humanized MAb KD-247 is suitable not only for use as a passive immunization antibody for the prevention of immunodeficiency virus infection but also to passively transfer antibodies for immunotherapy. Using 18 primary HIV-1 isolates, we evaluate the neutralizing capacity of KD-247. We also assess its efficacy against *ex vivo* generation of HIV from the peripheral blood mononuclear cells (PBMCs) of four HIV-infected individuals. Finally, we examine whether KD-247 can suppress HIV-1 replication in monkeys.

MATERIALS AND METHODS

Passive transfer of KD-247 to monkeys followed by pathogenic virus challenge. All animals used in this study were mature, cycling, male cynomolgus monkeys (*Macaca fascicularis*) from the Tsukuba Primate Center, National Institute of Infectious Diseases (NIID), Japan. They were free of known simian retroviruses, herpesviruses, bacteria, and parasites. They were housed in accordance with the Guidelines for Animal Experimentation of the Japanese Association for Laboratory Animal Science under the Japanese Law Concerning the Protection and Management of Animals (1, 38) and were maintained in accordance with the guidelines set forth by the Institutional Animal Care and Use Committee of NIID, Japan. Once approved by an institutional committee for biosafety level 3 experiments, these studies were conducted at the Tsukuba Primate Center, NIID, Japan, in accordance with the requirements specifically stated in the laboratory biosafety manual of the World Health Organization (44a).

The pathogenic SHIV strain C2/1 is an SHIV strain 89.6 variant isolated by *in vivo* passage in cynomolgus monkeys (37). The original SHIV 89.6 strain was kindly provided by Y. Lu at the Harvard AIDS Institute (Boston, MA) (19, 32). Virus stocks of SHIV C2/1 were stored at -125°C and thawed just prior to use. The challenge stock was provided by K. Shinohara of the National Institute of Infectious Diseases, Tokyo, Japan. Cynomolgus monkeys injected intravenously with SHIV C2/1 showed high levels of viremia and marked $\text{CD4}^{+}\text{T}$ -cell depletion within 2 weeks after inoculation (1, 34, 35, 37). Naïve monkeys were intravenously administered 0, 15, 30, or 45 mg/kg of KD-247 along with either 45 mg/kg of purified normal human immunoglobulin (Nihon Pharmaceutical Co., Tokyo, Japan) or saline. Twenty-four hours after antibody transfer, the animals were intravenously challenged with 20 50% tissue culture infective doses (TCID_{50} s) of SHIV C2/1.

***In vitro* virus neutralization assays.** The primary clinical isolate HIV-1_{MNp} was kindly provided by J. Sullivan of the University of Massachusetts Medical School, Worcester, MA. The virus was confirmed to be neutralization resistant (5). Laboratory-adapted HIV-1_{89.6} and HIV-1_{MN} were obtained from the AIDS Research and Reference Reagent Program, National Institutes of Health, Rockville, MD. GHOST cell neutralization assays were performed as described previously (5, 38). Briefly, GHOST cells expressing either CXCR4 or CCR5 coreceptors were used as targets of HIV-1 infection. The cells were then analyzed by

FACSCalibur flow cytometry (Becton Dickinson, San Jose, CA). The same concentration of either purified normal human immunoglobulin consisting primarily of the IgG1 subclass (Nihon Pharmaceutical Co.) or saline was used as control.

Neutralization activities in monkey plasma were assayed by detecting the neutralizing titers in the assay measuring 100% neutralization against the challenge virus as described previously by Nishimura et al. (26). In brief, plasma samples were serially diluted and incubated with 100 TCID_{50} s of challenge virus, and M8166 cells were then incubated as previously described (26). The neutralization was expressed as the percent inhibition of simian immunodeficiency virus p27 antigen production in the culture supernatants (38, 39). Normal monkey plasma was used as a control.

PBMC-based virus neutralization assay. HIV-1_{MN} (H9/HTLV-III MN) was kindly provided by the AIDS Research and Reference Reagent Program, National Institutes of Health, Rockville, MD (45). The WHO primary isolates 92TH002, 92TH022, 92TH023 (all clade E), and 92TH014 (clade B') were used as virus stocks (12). The primary isolates HIV-1_{JR-CSF} and the CS and JCI series of HIV-1 isolates were provided by Y. Koyanagi (40) and Y. Okamoto (27). *In vitro* virus neutralization assays were performed as previously described (7, 12). Neutralization titers are expressed as either the concentration of serum IgG antibody or the reciprocal of the serum dilution that yielded a 50% (50% inhibitory concentration [IC_{50}]) or 90% (IC_{90}) reduction in HIV-1 p24 production over that seen in controls using purified serum IgG from healthy individuals or preimmune mouse sera.

***Ex vivo* virus neutralization assays.** The PBMCs of patients infected with HIV-1 were depleted of CD8^{+} cells by magnetic separation using polystyrene beads coated with anti-CD8 MAb (Dynabeads M-450 CD8; Dynal, Oslo, Norway). The negatively selected cells were stimulated with OKT3 antibody (1 $\mu\text{g}/\text{ml}$; Janssen-Kyowa, Tokyo, Japan) and subsequently cultured in the presence of interleukin-2 (20 U/ml; Boehringer, Mannheim, Germany) together with KD-247 (60 and 240 $\mu\text{g}/\text{ml}$). The amount of HIV-1 p24 antigen in the supernatant was determined by enzyme-linked immunosorbent assay (ELISA) (Dainabot, Tokyo, Japan). Approval by the ethical committee and written informed consent from all the human subjects were obtained according to the guidelines of the Ministry of Health, Labor, and Welfare, Japan, and to those of the Kumamoto University Medical School, Kumamoto, Japan.

Competitive PCR quantitation of SHIV RNA in plasma. Quantitative competitive reverse transcription-PCR was performed as described previously by Piatak et al. (30), with both the substitution of a different competitor RNA and a different DNA template (35). The detection limit of this assay was 500 RNA copies/ml in monkey plasma.

Flow cytometric evaluation of cell surface antigen expression and absolute cell count. Mouse MAbs conjugated with either fluorescein isothiocyanate, phycoerythrin (PE), PE-Cy5, or peridinin chlorophyll protein were used in flow cytometric analyses to detect cellular expression of monkey CD3 (NF-18; BioSource International Inc., Camarillo, CA), human CD4 (Nu-TH/1; Nichirei Co., Tokyo, Japan), CD8 (SK-1; Becton Dickinson & Co., San Jose, CA), and CD95 (CH11 and 7C11; Becton Dickinson) (30). To determine absolute cell counts, samples of whole blood were analyzed following the addition of fluorescein isothiocyanate-conjugated anti-CD3 (BioSource), PE-conjugated anti-CD4 (Becton Dickinson), and peridinin chlorophyll protein-conjugated anti-CD8 (Becton Dickinson) MAbs as previously described (35).

Plasma concentration of KD-247. HIV-1 V3 peptide-based ELISA was used for quantification of KD-247 antibody. In brief, 96-well ELISA plates (Maxisorp; Nunc A/S, Roskilde, Denmark) were coated with 100 μl of a KD-247 antigen peptide (SP1 [YNKRRKRIHIGPGRAFYTTCNC]) per well in 50 mM carbonate buffer (pH 9.3) at 1 $\mu\text{g}/\text{ml}$ overnight at 4°C . KD-247 was diluted to concentrations ranging from 2.5 to 40 ng/ml as a reference. Bound KD-247 was detected with a peroxidase-conjugated anti-human IgG MAb (in-house preparation; The Chemo-Sero-Therapeutic Research Institute). The concentrations of KD-247 in the plasma of monkeys were determined using a calibration curve (SOFTmax; Molecular Devices Co., Menlo Park, CA).

Statistical analysis. The plasma concentrations at various data points postdose were applied to a two-compartment model using an automatic pharmacokinetic analysis program (nonlinear least-squares method), and pharmacokinetic parameters were calculated.

RESULTS

Neutralization ability of the humanized antibody KD-247 against a panel of primary isolates as determined by a PBMC-based study. In the initial series of the study, we showed that

TABLE 1. PBMC-based neutralization of primary and laboratory isolates by KD-247^a

Isolate	Env V3 sequence ^b		GHOST cell	KD-247		447-52D IC ₅₀ ^c
				IC ₉₀	IC ₅₀	
Laboratory isolates, clade B						
HIV-1 _{MN}	CTRPNYNKRKRRIHI	GPGRAFYTTKNIIGTIRQAHC	X4	1	0.1	0.1
HIV-1 _{SF2}	-----N-T-G----	-----A-EK-V-D-----	X4	5	1.0	1.0
HIV-1 _{89.6}	-----N-T-R-LS-	-----ARR----D-----	R5/X4	2.5	0.2	>10
Primary isolates, clade B						
HIV-1 _{JR-CSF}	----SN-K--S----	-----GE---D-----	R5	5	0.4	>10
HIV-1 _{CS2-2}	-----N-T--S--M	---K-----GD---N---Y-	R5	>50	>50	ND
HIV-1 _{CS3-5}	---I-N-T--S----	-----A-GE---N-K----	R5	10	1.4	ND
HIV-1 _{CS4-4}	-I---N-T--G----	-L--WK--A-G--N-----	R5/X4	>50	>50	ND
HIV-1 _{CS6-6}	--G--N-T--S-R-QR	-----V-IGK--NM-----	R5	>50	>50	ND
HIV-1 _{CS6-8}	-I---N-T--G----	-----A-D---N-----	R5	8	1.2	ND
HIV-1 _{JCI-1}	----HKTI-----	-----Q-E-N-----	X4	5	0.4	ND
HIV-1 _{JCI-2}	----SN-T-R----	-----RQ--R-D-----	X4	4	0.2	ND
HIV-1 _{JCI-3}	----N-I--H----	-----RG--RD--K----	R5	10	0.6	ND
HIV-1 _{JCI-5}	-----T--G----	-----V--G--RD--K----	X4	4	0.2	ND
HIV-1 _{JCI-6}	----SN-T-R----	-----S--A-Q-RGD-----	X4	6	0.7	ND
HIV-1 _{JCI-9}	-----T--G----	-----V--G--RD--K----	R5	21	1.6	ND
HIV-1 _{JCI-11}	-----TS-G-R-	-----ASER--RD--K----	R5	34	3.2	ND
HIV-1 _{JCI-22}	----N-I--H----	-----RG--RD--K----	R5	12	1.2	ND
Primary isolates, clade B'						
HIV-1 _{92TH1014}	----N-T--S-PL	----W--GQ--D-----	R5	8	0.9	>1.5
Primary isolates, clade E						
HIV-1 _{92TH1002}	----SN-T-TS-T-	---QV--R-GD---D--K-Y-	R5	>50	>50	ND
HIV-1 _{92TH1022}	----SN-T-TS-T-	---QV--R-GD---D--K-Y-	R5	>50	>50	>10
HIV-1 _{92TH1023}	----SN-T-TS-N-	---QV--R-GD---D--K-Y-	R5	>50	>50	ND
SHIV-B						
SHIV 89.6PD	----N-T-R-LS-	-----ARR----D-----	R5/X4	5	0.5	ND
SHIV C2/1	----N-T-E-LS-	-----ARR----D-----	R5/X4	5	0.5	ND

^a The HIV-1 sequences were confirmed by proviral DNA sequencing of virus-infected cells.

^b Dashes indicate sequence homology to HIV-1_{MN}, and spaces represent the presence of a deletion.

^c ND, not done.

sequential immunization with synthetic V3 peptides from representatives of primary HIV-1 clade B isolates generated cross-reactive antisera and produced a high-affinity humanized MAbs, KD-247, directed against the tip of the HIV-1 V3 domain, PGR. Furthermore, the humanized antibody more effectively neutralized several primary isolates of HIV-1 clade B than did previously reported neutralization antibodies (8a, 10, 23, 27). To further analyze the divergence of the cross-neutralization ability of the antibody by a PBMC-based HIV-1 neutralization assay, we used a panel of a total of 23 immunodeficiency viruses: 18 primary isolates of HIV-1 clade B, clade B', and clade E viruses; 3 laboratory HIV-1 clade B viruses; and 2 highly pathogenic SHIVs (Table 1). The KD-247 antibody effectively neutralized HIV-1_{MN}, HIV-1_{SF2}, and HIV-1_{89.6}, containing the consensus V3 sequence of HIV-1 clade B, IGPGRAFVY, with an IC₉₀ and IC₅₀ from 1 to 5 and from 0.1 to 1.0 μg/ml, respectively (Table 1, laboratory isolates, clade B). We next sought to assess whether the neutralization of primary isolates by KD-247 required a matching neutralization sequence motif. As expected, KD-247 effectively neutralized primary CCR5-tropic clade B and B' isolates (IC₉₀ and IC₅₀ from 5 to 34 and from 0.4 to 3.2 μg/ml, respectively) and all four of the CXCR4-tropic clade B isolates (IC₉₀ and IC₅₀ from 4 to 6 and from 0.2 to 0.7 μg/ml, respectively) with matching IGPGR

or V3 tip sequences. Thus, CCR5-tropic isolates with an IC₉₀ of a mean concentration of neutralization antibody of 13.5 μg/ml were more than 2.8 times less sensitive to the neutralization by KD-247 than primary CXCR4-tropic isolates with a mean IC₉₀ of 4.8 μg/ml. In contrast, the neutralization-resistant virus CS2-2 did not match the neutralization sequence motif, and the CS6-6 virus showed a QR insertion in the V3 tip sequence. The HIV-1 isolates containing a glutamine (Q) residue at position 20 in the V3 region, such as those of subtype E, were also resistant to neutralization by KD-247. Therefore, KD-247 effectively neutralizes both the CCR5- and CXCR4-tropic primary isolates with matching neutralization motifs.

Ex vivo suppressive effects of KD-247 on the generation of HIV-1 quasispecies from PBMCs of HIV-infected individuals.

To fully assess the antiviral efficacy of KD-247, we next sought to determine whether it would suppress the generation of HIV-1 from PBMCs of HIV-infected individuals and whether it would do so as efficiently as an established anti-V3 humanized antibody, CB1 (23). As shown in Table 2, we investigated the effect of KD-247 at concentrations of 60 and 240 μg/ml on the ex vivo generation of HIV-1 using CD8⁺-T-cell-depleted PBMC cultures from four Japanese individuals infected with HIV-1 clade B (Env V3 sequence in Table 2). In the presence of KD-247 at concentrations of 60 and 240 μg/ml, the gener-